HHS Public Access

Author manuscript

Pflugers Arch. Author manuscript; available in PMC 2022 September 01.

Published in final edited form as:

Pflugers Arch. 2021 September ; 473(9): 1469–1491. doi:10.1007/s00424-021-02548-9.

Transmission at rod and cone ribbon synapses in the retina

Wallace B. Thoreson[1]

[1]Truhlsen Eye Institute, Departments of Ophthalmology & Visual Sciences and Pharmacology & Experimental Neuroscience, University of Nebraska Medical Center, Omaha, NE 68198, USA

Abstract

Light-evoked voltage responses of rod and cone photoreceptor cells in the vertebrate retina must be converted to a train of synaptic vesicle release events for transmission to downstream neurons. This review discusses the processes, proteins, and structures that shape this critical early step in vision, focusing on studies from salamander retina with comparisons to other experimental animals. Many mechanisms are conserved across species. In cones, glutamate release is confined to ribbon release sites although rods are also capable of release at non-ribbon sites. The role of non-ribbon release in rods remains unclear. Release from synaptic ribbons in rods and cones involves at least three vesicle pools: a readily releasable pool (RRP) matching the number of membrane-associated vesicles along the ribbon base, a ribbon reserve pool matching the number of additional vesicles on the ribbon, and an enormous cytoplasmic reserve. Vesicle release increases in parallel with Ca^{2+} channel activity. While the opening of only a few Ca^{2+} channels beneath each ribbon can trigger fusion of a single vesicle, sustained release rates in darkness are governed by the rate at which the RRP can be replenished. The number of vacant release sites, their functional status, and the rate of vesicle delivery in turn govern replenishment. Along with an overview of the mechanisms of exocytosis and endocytosis, we consider specific properties of ribbon-associated proteins and pose a number of remaining questions about this first synapse in the visual system.

Keywords

Ribbon synapse; Photoreceptor cell; Vertebrate retina; Vision; Exocytosis

Introduction

Synaptic transmission from rods and cones to second-order retinal neurons is a key early step in the conversion of light responses into a neural code for vision. The task of this synapse is to convert light-evoked changes in membrane voltage into a sequence of synaptic vesicle release events. The properties of transmission at this first synapse in the retina shape visual capabilities in many fundamental ways [199]. For example, transmission at photoreceptor synapses acts as a bandpass filter [5, 230, 244]. Non-linearity in transmission at cone synapses preferentially enhances bipolar cell responses to small contrast changes

✉Wallace B. Thoreson, wbthores@unmc.edu.

Conflicts of interest The author declares that there is no conflict of interest.

[210]. Non-linear properties of transmission at rod synapses also filter out small noisy signals to increase the reliability of rod bipolar cells in detecting single photon responses [71]. Properties of release improve the detection of light decrements [106] and initiate the coding of changes in contrast vs. luminance [9, 158]. Modification of release by feedback from horizontal cells to cones yields spatiotemporal filtering that improves edge detection [212]. Inhibitory feedback from horizontal cells to cone synapses is also critical for performing spectral comparisons [211].

Our understanding of the mechanisms of release at photoreceptor synapses has come from studies using a number of animal models. Because of the relatively large size of its photoreceptor cells, salamander retina has served as a particularly useful model system. This review summarizes our understanding of photoreceptor synaptic function, focusing on results obtained in salamander retina with comparisons to results obtained in other animal models.

Anatomy and molecular composition of rod and cone ribbon synapses

Photoreceptor cell anatomy

Rod and cone photoreceptor cells consist of two largely independent compartments, inner and outer segments, separated by a thin non-motile cilium (Fig. 1a). The outer segment is specialized for phototransduction [7, 31, 69] while the inner segment contains ion channels that shape the light response along with the metabolic and synaptic machinery. A cluster of many mitochondria sits in the outer region of the inner segment just beneath the connecting cilium. These mitochondria provide ATP needed to sustain the activity of Na/K-ATPases as they work to counter the continuous influx of Na^+ ions through cGMP-gated cation channels in the outer segment that remain open in darkness [104, 160]. The buffering of Ca^{2+} by mitochondria also segregates Ca^{2+} changes in the inner segment from changes in the outer segment [74, 120, 213].

In mammalian retina, the synaptic terminals of rods and cones contain their own mitochondria to fuel transmission. However, the synaptic terminals of rods and cones in avascular retinas, including amphibians, lack mitochondria. These instead rely on energy supplied by mitochondria in the inner segments. In these animals, the mitochondria generate phosphocreatine to escape consumption by ATPases in the inner segment, allowing it to diffuse to the synaptic terminal where creatine kinase converts it to ATP [102].

Anatomy of photoreceptor ribbon synapses

Perhaps the most notable ultrastructural feature in the synaptic terminals of rods and cones is an electron-dense structure known as the ribbon [57] (Fig. 1b). In cross-section, ribbons appear as dark bars jutting into the cytoplasm perpendicular to the plasma membrane. In three dimensions, ribbons form flat planar structures with a thickness of ~ 35 nm [168, 193, 200]. Glutamate-filled vesicles attach to the ribbon surface in a hexagonal array. Each vesicle is tethered to the ribbon by 3–5 fine filaments [223]. Beneath each rod and cone ribbon rests a trough-shaped structure known as the arciform density (Fig. 1b).

Rod ribbons are generally larger than cone ribbons [168, 200]. In mouse and salamander rods, ribbons extend ~ 1 μm into the cytoplasm and ~ 1 μm along the membrane. Ribbons of mouse rods curl around the synaptic invagination, forming a horseshoe-shaped profile [81, 125, 173, 193, 250]. Mouse rods typically have only a single ribbon [41] but cat and primate rods often have two ribbons within each invagination [149]. Salamander rods can have as many as 3 terminals with each terminal possessing an average of 4 ribbons, yielding an overall average of ~ 7 ribbons per rod [222, 233].

Cone ribbons typically have dimensions of a few hundred microns along each side [3, 163, 168]. Unlike mouse rods that have only a single ribbon, cones have multiple ribbons with 10–15 apiece in mouse and an average of 13 apiece in salamander [19, 112, 163]. Ground squirrel cones [127] and foveal cones of primates have ~ 20 ribbons apiece, with the number of ribbons in primate cones increasing towards the periphery to ~ 40 ribbons apiece [48, 114].

Ribbons are also found in other sensory neurons that encode graded membrane potential changes. Retinal bipolar cells have smaller plate-like ribbons while hair cells of the auditory and vestibular apparatuses have small, ovoid ribbons [153].

Rods and cones form synapses with dendrites of second-order bipolar and horizontal cells. In both rods and cones, ribbons rest at the apex of an invagination into the synaptic terminal membrane (Fig. 1b). Mouse rod ribbons typically contact two ON-type rod bipolar cells [24] but as many as four rod bipolar cell dendrites may enter each invagination in primate rods [85]. In cones, ON-type bipolar cell dendrites occupy the central position within the invagination whereas OFF-type bipolar cells make flat contacts at the base of the synapse just outside the invagination [91]. A few flat, basal contacts from cone bipolar cells can also be seen just outside the invagination in rods [128, 140]. Unlike mammals, central bipolar cell dendrites in salamander retina often come from OFF bipolar cells whereas ON bipolar cells often make basal contacts [123]. Flanking the central bipolar cell dendrites within the invagination is a pair of horizontal cell processes that can provide inhibitory feedback to rods and cones [23, 178, 207, 212]. Bipolar cell circuitry is reviewed in detail elsewhere [68].

Molecular constituents of synaptic ribbons

Proteomic analysis has identified many different proteins associated with ribbons, but the most prevalent is a transcript variant of CtBP2 known as ribeye [111, 224]. The two variants of CtBP2 share a common B domain but ribeye has an additional ribbon-specific A domain. The shorter, more ubiquitous form of CtBP2 is present in the nucleus of many cells [196]. The shared B domain of CtBP2 contains a transcriptional repressor as well as lysophosphatidic acid acyltransferase (LPAAT) but the role that these domains play, if any, at ribbon synapses is not known [190]. The core structure of each ribbon is formed from tens of thousands of ribeye molecules [185, 186, 252] with the ribbon-specific A domain apparently facing the center [137]. The laminar appearance of photoreceptor ribbons is consistent with this arrangement (see Fig. 6 in [122]) and the 35-nm thickness of photoreceptor ribbons matches the dimensions of two parallel rows of ribeye proteins [154].

The related protein CtBP1 is also associated with ribbons, but deletion of CtBP1 had only mild effects on rod synaptic structure and function in mouse retina [225].

In heterologous expression systems, ribeye molecules coalesce into spherical bodies, roughly similar in shape to hair cell ribbons [186]. Spherical synaptic bodies are also found in the terminals of photoreceptors from hagfish, a primitive jawless fish [98]. The formation of the planar structure of retinal ribbons requires interactions with piccolino, a ribbon-specific piccolo splice variant [154]. The putative motor protein myosin Va [184] may also help with the construction of planar ribbons [129].

Interactions between adjoining ribeye molecules are sensitive to NADH and it is thought that metabolic changes in NADH levels that accompany changes in light and dark might be the mechanism controlling disassembly of rod ribbons with illumination in day-time and their re-assembly at night [1, 2, 59, 137, 186, 195]. Ribbons also disassemble during hibernation in ground squirrel cones and then rapidly re-assemble after waking [144, 178].

Kif3A is a kinesin motor protein associated with ribbons [155, 220] fueling speculation about motor-driven movement of vesicles. However, motor functions of Kif3A typically require heteromeric association with Kif3B or 3C [169], and these do not appear to be present at ribbons [111, 224]. Elimination of Kif3A causes photoreceptor degeneration but this appears to be a result of disturbed ciliary transport processes [108]. Furthermore, the release of vesicles on the ribbon can proceed without ATP suggesting that an ATP-dependent motor is not required for movement along the ribbon [95].

Composition and function of the arciform density

The trough-like arciform density that rests beneath each photoreceptor ribbon (Fig. 1b) is not found at other ribbon synapses. It is a complex of multiple proteins including bassoon, Munc13–2, Rim2, and ERC2/CAST1 [30, 49, 58, 88, 220, 221]. Loss of bassoon leads to detached ribbons and diminished synaptic transmission from rods [10, 63]. (We return later to discuss differences in the effects of bassoon and Ribeye knockouts.) After deleting CAST1, ribbons remain attached but the size of the active zone is reduced [220].

In addition to the particular functions performed by specific proteins that constitute the arciform density, a more general function is that it may shape the diffusion of Ca^{2+} ions entering channels positioned just beneath it. Simulations of salamander cones suggested that a diffusion barrier created by the arciform density could limit the spread of Ca^{2+} and thereby limit the ability of an open Ca^{2+} channel to trigger release of multiple vesicles [20]. This could in turn help to ensure a linear relationship between I_{Ca} activation and release [20, 113]. However, rods and cones are also capable of multivesicular release, and it was proposed for hair cell ribbons that constraining Ca^{2+} diffusion beneath the ribbon can enhance the likelihood of multiquantal release by promoting local buffer saturation [82].

Exocytotic proteins

Like most neurons, exocytosis of glutamate-filled vesicles at rod and cone ribbons synapses involves SNARE proteins. The vesicle-associated SNAREs, synaptobrevin and SNAP-25, are the same as those used at other synapses [238], but the t-SNARE on the plasma

membrane, syntaxin 3B, is not used as widely [53, 151]. As discussed later, this SNARE protein promotes vesicle-vesicle fusion on the ribbon [92] but may also play other roles [53, 131].

In addition to this atypical SNARE protein, rods and cones also use complexins 3 and 4 rather than the more commonly used isoforms 1 and 2 [177]. The properties conferred by complexins 3 and 4 are qualitatively similar to properties of complexins at other mammalian synapses, e.g., limiting spontaneous release and facilitating evoked release, but they may also play a distinct role in regulating replenishment of vesicles to the ribbon [13, 152, 226, 228].

What are the molecular constituents of filaments that tether vesicles to the ribbon?

It was suggested that interactions between rab3A and partner molecules on the ribbon such as Rim (rab-interacting molecule) might form the fine tethers that attach vesicles to the ribbon [224]. Each vesicle has 10 or more copies of rab3A [245], which would support the observed number of tethers. More convincingly, peptides that interfere with rab3A function impaired vesicle replenishment [219]. However, while it was originally thought that Rim1 was present along the ribbon face [220], it was later shown that Rim1 antibody labeling on the ribbon was due to cross-reactivity with piccolino [133]. Rim2 is present at the arciform density but not along the ribbon face. The Rim2 variant in photoreceptors also exhibits weaker binding to rab3A than full-length Rim2 [133]. Although rab3a is not likely to interact with Rim proteins along the face of the ribbon, it may interact with other ribbon-associated proteins, such as rabphilin [224].

Release at rod and cone synapses

Ca^{2+} channels

Rods and cones maintain a relatively depolarized membrane potential in darkness, hyperpolarizing in response to increased light intensity and depolarizing to decreased intensity. Rods and cones lack voltage-gated Na^+ channels and so light-evoked voltage changes spread passively from the outer segment to the synaptic terminal, modified by voltage-and Ca^{2+}-dependent ion channels along the way [229]. These voltage changes regulate the activity of synaptic Ca^{2+} channels to control release of glutamate-filled synaptic vesicles [see review by 164], thereby converting light-evoked voltage changes into a train of vesicle release events. Unlike conventional synapses that use N or P type Ca^{2+} channels, ribbon synapses rely on L-type Ca^{2+} channels [187, 213, 246]. Photoreceptors use a particular type of L-type channel, $Ca_V1.4$, which shows minimal Ca^{2+}- and voltage-dependent inactivation [22, 115, 142, 164, 240]. Over 100 mutations in $Ca_V1.4$ that have been identified, most of which cause some form of congenital stationary night blindness (CSNB) by impeding transmission of signals from rods [251].

Salamander cones possess 50–75 channels/ribbon or 3–4 channels for every vesicle [20]. The single channel properties of Ca^{2+} channels in salamander rods are similar to other L-type channels with a peak open probability approaching 0.3 and single channel conductance in Ba^{2+} of 20 pS [214] (Fig. 2a). By contrast, single channel recordings from heterologously

expressed $Ca_V1.4$ channels recorded under similar conditions showed a single channel conductance of only 9 pS and peak open probability of 0.05–0.1 [32, 64]. Given these values, a macroscopic I_{Ca} in mouse cones of 45 pA would require 3500–7000 channels/cone or 200–700 channels per ribbon.

The lack of Ca^{2+}-dependent inactivation in $Ca_V1.4$ channels is due to an autoinhibitory domain in the C-terminus that competes with binding of apo-CaM (Ca^{2+}-free CaM). Because apo-CaM and the autoinhibitory domain both compete for the same binding site, elevated CaM levels can enhance Ca^{2+}-dependent inactivation. Phosphorylation can also promote apo-CaM binding and thereby enhance inactivation [87, 124, 182, 206]. In addition, some splice variants of $Ca_V1.4$ lack this autoinhibitory domain altogether [87]. Mechanisms such as these may explain the slow Ca^{2+}-dependent inactivation seen in salamander rods (τ = 1.7s) [50, 172].

In addition to genuine Ca^{2+}-dependent inactivation, depletion of Ca^{2+} ions from the synaptic cleft during maintained activation can also limit the amplitude of I_{Ca}. Similar to calyceal synapses [28, 197], the continued influx of Ca^{2+} ions at invaginating rod synapses as they remain depolarized in darkness can deplete the limited number of Ca^{2+} ions available in the tiny volume of the synaptic cleft causing a slow, overall decline in I_{Ca} [172].

Along with differences in the degree of Ca^{2+}-dependent inactivation, some of the more than 20 splice variants of $Ca_V1.4$ differ in their voltage-dependence [87]. This variation can extend the range over which light-evoked voltage changes regulate channel activity. Voltage-dependence of $Ca_V1.4$ is also regulated by association with a Ca^{2+}-binding protein CaBP4 that shifts the voltage-dependence of $Ca_V1.4$ to more negative potentials, providing a better match to the voltage range attained during rod and cone light responses [86].

$Ca_V1.4$ channels form a complex with intracellular β2 subunits and extracellular α2δ4 subunits [15, 249]. These subunits play a role in trafficking to the membrane but also regulate channel activity [65]. A common variant of the β2 subunit in human retina enhances voltage-dependent inactivation [124]. α2δ4 subunits are anchored to the extracellular membrane surface by glycosylphosphatidylinsolitol (GPI) links [56]. Interactions between α2δ4 and another extracellular protein, ELFN1, are critical for proper formation of rod synapses during development [112, 242]. Structural elements of the alpha subunit $Ca_V1.4$, independent of its ability to conduct Ca^{2+}, also play a role in stabilizing rod synapses [136].

Ca^{2+}-activated chloride channels

Ca^{2+}-activated Cl^- channels are localized to synaptic terminals of rods and cones, but distributed more diffusely throughout the terminal than Ca^{2+} channels [135, 146]. The Ca^{2+}-activated Cl^- channels in rods appear to be Ano2 channels while those of cones are a different subtype [55, 201]. In addition to regulating transmembrane voltage, chloride ions that move through these channels can regulate the open probability of L-type Ca^{2+} channels by interacting with anion-binding sites on the intracellular C-terminus and the beta subunit [11, 213, 214]. The chloride equilibrium potential in rods is relatively depolarized at ca. − 20 mV so activation of Ca^{2+}-activated Cl^- channels at or below the resting membrane potential promotes an efflux of Cl^- that can in turn reduce Ca^{2+} channel activity [209]. This negative

feedback interaction may provide a mechanism for adaptation and help to limit regenerative activation of Ca^{2+} channels. In ground squirrel cones with a resting membrane potential of ~ − 50 mV, E_{Cl} also has a relatively depolarized value of ~ − 30 mV [205], supporting the possibility of similar negative feedback interactions. In non-mammalian cones, E_{Cl} is closer to the resting membrane potential in darkness suggesting more limited effects of this mechanism to regulate Ca^{2+} channel activity in these cells [208].

Voltage-dependence of exocytosis

In most species, the resting membrane potential of rods and cones in darkness is around − 40 mV, close to the activation midpoint for $Ca_V1.4$ channels in vivo (Fig. 2c) [14, 80]. The limited inactivation of $Ca_V1.4$ channels allows them to remain active at the dark potential, smoothly altering activity to continuously encode light-evoked changes in membrane potential. The resting potential is near the steepest part of the activation curve, maximizing sensitivity to small changes in membrane potential. Channel activity diminishes with the membrane hyperpolarization evoked by light. The non-linear nature of I_{Ca} activation contributes to a greater change in cone output produced by small changes in contrast compared to larger contrast changes that produce larger voltage excursions [210]. With a very bright flash, the membrane can hyperpolarize to a level at which there is virtually no Ca^{2+} channel activity. This contributes to the “clipping” of rod signals in second-order neurons seen with bright flashes, in which the initial, transient component of the hyperpolarizing rod response evoked by bright light is transmitted quite poorly [8, 217].

Many substances can modulate Ca^{2+} channels at rod and cone synapses [164, 229]. One notable difference from Ca^{2+} channels at most other synapses is that the normal resting membrane potential in photoreceptors is near the midpoint for I_{Ca} activation. One consequence of this is that small differences in resting membrane potential between cells can cause significant cell-to-cell differences in sensitivity to the same light-evoked response. This arrangement also means that the activity of photoreceptor Ca^{2+} channels is unusually sensitive to small shifts in activation along the voltage axis. Thus, the local ionic environment can influence voltage-dependence significantly. For example, lowering the extracellular concentration of cations (e.g., divalent cations or protons) reduces positive charge on the outer membrane surface, altering the local electrical field experienced by Ca^{2+} channels and allowing them to be activated more easily [159, 167]. Thus, depletion of Ca^{2+} or H^+ from the synaptic cleft produces a negative (leftward) shift in the activation curve for I_{Ca}. Changes in anion levels can also alter membrane surface charge, shifting activation in the opposite direction from changes in cation levels [216].

The retina has exploited the sensitivity of Ca^{2+} channels to protons [103, 159] as a means of regulating photoreceptor synaptic output [16, 17]. The co-release of protons with glutamate from synaptic vesicles causes rapid, transient inhibition of presynaptic I_{Ca} in cones [61, 101]. And while other mechanisms may contribute, an essential component of inhibitory feedback from horizontal cells to cones and rods involves proton-mediated changes in Ca^{2+} channel activation [212]. The hyperpolarization of horizontal cells in response to light alkalinizes the synaptic cleft, relieving proton-mediated inhibition of I_{Ca} and, more importantly, shifting I_{Ca} activation leftward to more negative potentials [35, 97, 236, 237,

241]. Together, these effects of horizontal cell feedback promote recovery of I_{Ca} when surrounding horizontal cells are hyperpolarized (e.g., by an increase in spatially-averaged luminance). And because the extracellular environments of invaginating synapses remain relatively isolated from one another, individual cone ribbons can be regulated independently by dendrites of different horizontal cells, fine-tuning the feedback signal in response to local changes in illumination [43, 80].

Ribbon-to-ribbon differences in ionic content arising from differences in the distribution of channels and transporters may also contribute to differences in the voltage-dependence of Ca^{2+} channels at different ribbons in the same cell [80]. The presence of multiple ribbons that differ somewhat in their sensitivity to light-evoked voltage changes, either because of the expression of different splice variants [87] or local differences in the ionic environment, may extend the voltage range for synaptic output available to a cone.

Release from cones occurs exclusively at ribbons

In collaboration with Dr. David Zenisek, we studied the role of ribbons in release using a technique known as fluorescence-activated laser inactivation (FALI). For these experiments, we introduced a fluorescein-conjugated peptide that selectively binds to ribeye into rods or cones through a patch pipette. The free radicals released upon activation of the fluorophore by bright laser light causes highly localized damage to the ribbon and nearby proteins. Including high antioxidant concentrations minimizes non-selective damage. Acutely damaging salamander cone ribbons in this way reduced both fast and slow components of release from cones equally, indicating that both forms of release occur at ribbons [194]. Lowering Ca^{2+} buffering and inhibiting Ca^{2+} extrusion to promote the spread of Ca^{2+} to non-ribbon sites also did not reveal any additional slower components to release from cones [233]. These data indicated that release from salamander cones occurs only at their ribbons. Evidence from ground squirrel cones where ribbons re-assemble rapidly after awakening from hibernation indicates an essential role for ribbons in mediating release [144]. Another study in ground squirrel retina analyzed miniature excitatory post-synaptic currents recorded simultaneously in different classes of bipolar and horizontal cells. The different cell types differed in distance from ribbon release sites, and it was found that synaptic events in more distant cells were smaller and showed slower kinetics. This indicated that the ribbon was the sole source of glutamate for all of the observed events [62]. The exclusive use of ribbons in cones differs from rods (see below) and retinal bipolar cells [143, 148] that are also capable of release at ectopic, non-ribbon sites.

Vesicle pools at ribbon synapses

The vesicle pools involved in release from cone ribbons in salamander retina have been analyzed using both membrane capacitance recordings and paired recordings from cones and horizontal cells (Fig. 1b) [19, 170]. As illustrated in Fig. 1d, stimulating a cone with a long depolarizing step evokes a fast inward current in horizontal cells that rapidly subsides to a smaller, more sustained current. There is little saturation or cross-desensitization among neighboring glutamate receptors so miniature post-synaptic currents evoked by release of individual vesicles sum linearly with one another at the cone-horizontal cell synapse in salamander retina [33, 36]. One can therefore measure the total amount of release during

the test step by integrating the post-synaptic current to measure the total charge transfer (Fig. 1e). This approach revealed three components to release at salamander cone synapses: (1) A fast, transient component released within a few milliseconds consisting of ~ 15–20 vesicles/ribbon [19, 218] (dotted green trace, Fig. 1e). This represents a readily releasable pool (RRP) of vesicles and matches the number of ribbon-associated vesicles that contact the plasma membrane along the bottom two rows of the ribbon (yellow vesicles, Fig. 1c). Ground squirrel cones have a similar size RRP [77]. (2) With maintained depolarization, a second component consisting of ~ 90 vesicles per ribbon can be depleted from salamander cones within a few hundred milliseconds [19, 105] (dotted blue trace, Fig. 1e). The size of this secondary reserve pool matches the remaining number of vesicles further up the ribbon (blue vesicles, Fig. 1c). (3) After emptying these first two pools, release can be maintained at a linear rate more or less indefinitely (dotted gray trace, Fig. 1e), likely reflecting replenishment of ribbon-associated vesicles from the cytoplasmic pool [19]. Using similar approaches, we found that the RRP in salamander rods averages ~ 25 vesicles/ribbon [233]. Membrane capacitance recordings from mouse rods suggest an RRP of ~ 90 vesicles, also consistent with the number of membrane-associated vesicles at the base of mouse rod ribbons [76].

Graded voltage changes in rods and cones are converted to discrete vesicle release events. The number of discriminable intensities that can be encoded is thus limited by the size of the releasable pool and release rate [106, 199]). One way that cones address this limitation is by distributing release over many different ribbons, thereby increasing the effective size of the releasable pool. In addition, as mentioned earlier, differences in the voltage-dependence among ribbons can expand the intensity range over which an individual cone can encode voltage changes [80].

Ca^{2+}-dependence of exocytosis

The quantal hypothesis of synaptic transmission postulates that the post-synaptic current is a product of three variables, $n \times P \times Q$, where n = the number of vesicles in the RRP, P = probability that a vesicle in that pool will be released, and Q = quantal content of a single vesicle. While we initially thought that stronger stimulation of cones might recruit more distant release sites and thus increase N, our analysis of post-synaptic currents in salamander cones showed that voltage-dependent changes in release were determined solely by changes in P and that the size of the RRP appears fixed [218]. A recent study came to a similar conclusion for ribbon-mediated release from mouse rods [76]. While cytoplasmic glutamate levels can influence Q, changes in transporter activity or cytosolic glutamate levels are generally too slow to encode light responses directly [21].

The number of open Ca^{2+} channels determines release probability, P, and release rises linearly with increases in I_{Ca} [215]. One important factor contributing to this linearity is that release at cone ribbons is regulated by highly localized Ca^{2+} changes within nanodomains < 100 nm from $Ca_V1.4$ Ca^{2+} channels [146]. As discussed earlier, this behavior may require the diffusion barrier formed by the arciform density. As I_{Ca} increases, more channels are activated allowing a larger number of vesicle release sites to be engaged. The amount of release thus rises in parallel with channel activity. The $Ca_V1.4$ Ca^{2+} channels that control

release appear to be grouped in small clusters beneath the ribbon [134, 175] and release of a single vesicle in the RRP of salamander cones can be triggered by 2–3 Ca^{2+} channel openings [20]. Salamander rods are a bit less efficient, requiring the opening of 3–5 Ca^{2+} channels to trigger release of a vesicle [233].

Sensitivity of the exocytotic Ca^{2+} sensor molecules to intracellular Ca^{2+} levels may also contribute to linearity in release [66, 180, 215]. Ca^{2+} sensitivity of release is most accurately measured using caged Ca^{2+} compounds to abruptly elevate Ca^{2+} levels throughout the cell by photolysis with a bright UV flash. Photolytic uncaging elevates Ca^{2+} levels evenly throughout the cell so that average changes in cytoplasmic Ca^{2+} levels are the same as those experienced by the exocytotic Ca^{2+} sensor just beneath the plasma membrane. Using this technique, we measured release kinetics from the exocytotic rise in membrane capacitance accompanying vesicle fusion and by the kinetics of post-synaptic currents evoked in horizontal cells during paired recordings. Consistent with earlier findings [180], our results showed that the sensor in salamander rods and cones has a very high sensitivity to Ca^{2+}, with a threshold of only a few hundred nanomolar. There is also evidence for a lower affinity sensor in salamander cones [118]. Our studies showed that the high affinity sensor has an intrinsic Ca^{2+} cooperativity of 2–3 [66, 215]. The high affinity and low cooperativity of this sensor differs from most synapses that typically show lower affinity and higher cooperativity (n = 4–5). Simulations indicated that the high affinity of rod and cone sensors arises from a slow off-rate for Ca^{2+} unbinding [66]. This would extend the time that the sensor is partially occupied with Ca^{2+} during which binding of one or two additional Ca^{2+} ions might be enough to evoke release. This property may also help to linearize the overall Ca^{2+} dependence of release at rod and cone synapses.

The exocytotic Ca^{2+} sensors that mediate fast release at most conventional synapses, synaptotagmin 1 (Syt1) and 2, are not found at photoreceptor synapses of salamanders or fish [27, 96] but Syt1 is present at rod and cone synapses in mammalian retina [72]. Selective genetic elimination of Syt1 from mouse cones totally abolished their release [79]. Eliminating Syt1 from mouse rods abolished fast, synchronous release evoked by brief stimuli but a slower component remained intact. One question is whether mouse rods and cones that use Syt1 also exhibit the high affinity and low Ca^{2+} cooperativity found in amphibians. It is generally thought that the cooperativity of n = 4–5 reflects the presence of 5 Ca^{2+}-binding sites in Syt1 so it would be interesting to know if this property is retained at Syt1 synapses of rods and cones.

Vesicle cycle at rod and cone ribbons

Influence of replenishment on kinetics

Figure 3 illustrates the key steps in the vesicle cycle at photoreceptor ribbon synapses. By analogy with the behavior of electrical capacitors, plate-like ribbons “charge” with vesicles along their surface in light when release is minimal (i.e., when photoreceptors are hyperpolarized). Ribbons can then discharge vesicles in a rapid burst when photoreceptors depolarize upon return to darkness [106]. The large burst of release during an abrupt return to darkness expands the number of discriminable intensities 2.7 fold [106]. This enhancement of release at light offset may be one mechanism that contributes to the greater

sensitivity of human observers to light decrements compared to increments [29]. After this initial burst, release slows to a rate governed by the rate at which vesicles descend the ribbon to re-occupy available release sites. The fraction of the RRP released at any given membrane potential is determined by the release probability and that is in turn determined by the fraction of open Ca^{2+} channels. At a constant membrane potential, the fraction of the RRP that that is available for replenishment (i.e., the number of empty release sites at the base of the ribbon) remains constant, neither growing nor declining [9]. This behavior in cones matches that of bipolar cells where the initial burst of release at light offset has been shown to provide a measure of the change in contrast, whereas the rate of sustained release provides a measure of luminance [158]. Slowing vesicle replenishment (by inhibiting endocytosis or using calmodulin inhibitors as described later) impairs the ability of the synapse to following flickering light stimuli showing that the rate at which vesicles can replenish release sites is important for shaping frequency response characteristics [230].

Post-synaptic factors also play a role in recovery and kinetics [60, 205]. For example, the time constant for presynaptic replenishment of the vesicle pool in ground squirrel retina is slower than the rate at which post-synaptic AMPA receptors in OFF bipolar cells show recovery [77]. At this synapse, post-synaptic receptors are saturated by glutamate well before the entire RRP is released and so restoring only a portion of the RRP can be sufficient to produce large post-synaptic responses, thereby speeding recovery of post-synaptic responses during replenishment.

In salamander retina, the situation appears different. At salamander cone synapses, there is a linear correlation between pre-and post-synaptic measurements of release over much of the response range [170]. In addition, post-synaptic currents evoked in horizontal cell by depolarizing stimulation of cones can be predicted from a simple linear sum of individual quantal release events [33, 36]. These capabilities arise because the glutamate released from each vesicle is separated sufficiently in space and time from other single vesicle release events at the same synapse [163]. This avoids the receptor saturation seen in ground squirrel OFF bipolar cells and provides enough time for AMPA receptors to recover from desensitization before another release event impinges on the same set of receptors [163].

Endocytosis

Rods and cones have enormous cytoplasmic pools of vesicles, much larger than those of conventional neurons that typically have only 100–200 vesicles per synapse. Terminals of salamander rods and cones contain ~ 80,000 and ~ 194,000 vesicles, respectively [191]. Even mouse rods with only a single ribbon possess 5800–7500 vesicles [250]. In addition, unlike conventional synapses where most vesicles are immobilized to the cytoskeleton by interactions with synapsin, photoreceptor and bipolar cell ribbon synapses lack synapsin [138] allowing 85% of the vesicles to move freely within the synapse [176]. This means that there is a huge pool of cytoplasmic vesicles readily available to replenish ribbon release sites and accommodate changes in release rate. Although capable of higher rates when maximally stimulated, sustained release rates in darkness in rods and cones appear to range from 10 to 20 v/s/ribbon, as measured by a number of different techniques [26, 94, 191]. However, even

at 10 v/s/ribbon, the entire pool of vesicles in a salamander rod terminal would be emptied after 45 min of darkness without vesicle recycling.

Endocytosis at rod and cone ribbon synapses involves both fast and slow retrieval mechanisms [51, 105, 231]. Fast retrieval has a time constant of a few hundred milliseconds and can be inhibited in rods by inhibiting the GTPase dynamin [231]. By contrast, the fast component of retrieval in salamander cones was insensitive to GTPase inhibitors [231]. Studies involving differences in the release and retrieval of large and small dye molecules suggested that this fast component may involve kiss-and-run mechanisms [243]. The slower component involves both clathrin-mediated endocytosis [192, 239] and clathrin-independent mechanisms. Key endocytic proteins involved in clathrin-independent retrieval at mouse rod synapses include dynamin 3, syndapin, calcineurin, endophilin, and synaptojanin [73, 99, 192, 239]. These proteins are enriched in the periactive zone surrounding the ribbon where endocytic vesicles arise after stimulation [73, 239].

In addition to replenishing the pool of available vesicles, endocytosis is needed to clear release sites of vesicular proteins and lipids deposited during prior fusion. This process is essential for restoring release sites to functional status. Imaging of single Ca^{2+} channels tagged with fluorescent quantum dots showed that immediately after vesicle fusion, the active zone briefly expands, thereby increasing the average distance between Ca^{2+} channels and release sites [145]. The active zone also expands after endocytosis is impaired (e.g., by the dynamin inhibitor, dynasore), presumably as a result of the additional, un-retrieved membrane. Increasing the distance between Ca^{2+} channels and release sites reduces release efficiency by increasing the number of Ca^{2+} channel openings needed to trigger release [147]. This may contribute to impaired fusion when endocytosis is blocked, but a more significant factor appears to be changes in the lipid and protein composition of the release site [244]. TIRF imaging of single vesicles showed that vesicles that descend the ribbon are released almost immediately or else dock at the membrane to await later release. However, when endocytosis was inhibited, fewer vesicles were released immediately and many of the docked vesicles turned around and retreated back up the ribbon, something that was almost never observed under normal conditions. These data suggested that endocytosis is needed to restore release site function, but inhibiting endocytosis did not impair vesicle docking. As mentioned above, slowing replenishment by blocking endocytosis also impaired the ability of second-order neurons to follow flickering light stimuli [244].

Glutamate refilling

After vesicles are retrieved by endocytosis, they must be refilled with glutamate. While this has not been measured directly in rods and cones, vesicle filling rates at central synapses show a time constant of ~ 15 s [100]. Vesicular glutamate uptake can influence kinetics at conventional synapses that possess many fewer vesicles [157], but rods and cones have a much larger repository of vesicles available for release while waiting for newly retrieved vesicles to be refilled. So, in the short run (seconds), refilling is not likely to be rate limiting for vesicle replenishment.

Ribbon replenishment

Vesicle replenishment rates are often measured using a paired pulse protocol. This protocol begins by applying a strong depolarizing test pulse from a holding potential where all Ca^{2+} channels are closed. The pulse amplitude and duration of this test pulse is chosen to release all of the vesicles in the RRP. After waiting a certain interval, a second test pulse is then applied to measure how much of the RRP has been replenished during that interval. By testing a range of interpulse intervals, vesicle replenishment in salamander cones was found to exhibit two components with time constants of ~ 600–800 ms and ~ 10 s (at room temperature) [105, 171, 218, 230]. The fast time constant for replenishment in ground squirrel cones shows a similar rate of recovery, with time constants of 450–700 ms (at 32 °C) [77]. In salamander retina, the slower replenishment mechanism is Ca^{2+}-independent whereas Ca^{2+} acting through calmodulin regulates the fast component [230]. Unpublished data from our laboratory suggests the fast component also involves CaMKII that is known to be associated with ribbons [111, 224]. Ca^{2+}/CaM acts to increase the proportion of vesicles that are replenished by the fast mechanism, but does not alter replenishment time constants [230]. This indicates that Ca^{2+} acts on the attachment process rather than individual vesicles. If Ca^{2+} acted on individual vesicles to alter their attachment probability, then the overall attachment probability would be a weighted average of Ca^{2+}-dependent and Ca^{2+}-independent attachment probabilities, yielding a single time constant that varied with Ca^{2+}. However, if Ca^{2+} acts on the ribbon to alter attachment, then this analysis predicts two time constants with Ca^{2+} varying the proportion of the two components, as found in the data [230].

Vesicle movement along ribbons

Each vesicle is attached to a ribbon by 3–5 fine tethers [223]. We discussed the possibility earlier that the tethers may represent interactions between rab3A on vesicles and a ribbon-associated protein [219, 224]. Similar to results from bipolar cells [132, 227], experiments in rods indicate that vesicles can attach anywhere along the face of the ribbon and move freely along its surface but are released only at sites along the base [222, 244]. If vesicles can move freely on the ribbon, then each individual tether must provide a relatively weak binding force. A strong tethering force would restrict lateral movements while a weak force allows individual tethers to detach and be replaced by another nearby tether. This can allow vesicles to move freely along the face of the ribbon while the combined force from multiple tethers remains sufficient to prevent vesicles from popping off the ribbon prior to fusion. Vesicles appear to migrate along the surface of the ribbon in a type of movement characterized as “crowd-surfing” [83]. Fusion of vesicles at the base of the ribbon creates vacancies that can be re-occupied by vesicles further up the ribbon. And because new vacant sites are only created at the base, vesicles will tend to diffuse passively from top to bottom without requiring active molecular motors [83], consistent with evidence that ribbon-associated vesicles can be released in the absence of ATP [95].

Vesicle priming

In addition to storing vesicles and regulating their delivery, ribbons play a role in priming vesicles to make them competent for release. After selectively damaging ribbons by FALI,

the existing RRP can be released but subsequent release of additional vesicles is impaired. Electron micrographs showed that although subsequent fusion was impaired by damage to the ribbon, vesicles were able to attach to the ribbon and occupy release sites along the base of the ribbon [194]. Together, these results suggested that the impairment was specific to an essential priming step. Further evidence for the importance of the ribbon in preparing SNARE complexes for release comes from experiments showing that use of a peptide to inhibit formation of SNARE complexes did not inhibit release of either the RRP or the slower component thought to reflect the ribbon-attached pool but impaired further replenishment [54]. These data suggest that SNARE complexes begin to form after vesicles attach to the ribbon, but before membrane association. Also consistent with the idea that vesicles are primed during descent are TIRF imaging experiments showing that vesicles arriving at ribbon-associated release sites are released almost immediately [46, 244]. This is illustrated in Fig. 4 that shows a dye-filled vesicle approaching a rod membrane and progressively brightening as it advances through the evanescent field generated by TIRF microscopy. The vesicle then fuses, disappearing within a single 40 ms frame as dye is released. Immediate fusion after reaching the membrane is analogous to “crash fusion” observed in neuroendocrine cells [235] and differs from synapses in bipolar cells and the calyx of Held where vesicles pause at the membrane for a few hundred milliseconds before release, presumably to await completion of a final priming step [110, 150, 253]. Furthermore, Munc13–2 and RIM proteins that prime vesicles at most other synapses do not appear to be necessary for priming vesicles at photoreceptor ribbon synapses, and the Rim2 variant in photoreceptors lacks interaction sites with Munc13–2 [49, 133]. Although Rim2 does not participate in vesicle priming, it is important for enhancing Ca^{2+} influx through Ca_V 1.4 Ca^{2+} channels [75].

Multivesicular release

A fundamental purpose of synaptic ribbons is to facilitate the ongoing release of multiple vesicles. In addition to maintaining release of vesicles during maintained depolarizing stimulation, rod and cone ribbons are also capable of the synchronized, simultaneous fusion of multiple vesicles [92]. We have studied the properties of individual release events at rod and cone synapses by recording post-synaptic currents in horizontal and OFF bipolar cells as well as by recording the presynaptic anion currents activated during glutamate re-uptake into photoreceptor cells [6, 67, 78, 89, 166]. In salamander rods and cones, release events measured in both ways show widely varying amplitudes but similar kinetics suggesting that they arise from the synchronized fusion of multiple vesicles [36, 52, 92]. While small, presumptive single vesicle fusion events are more common, ~ 1/3 of the spontaneous events in salamander rods involve synchronous multiquantal fusion [92]. In collaboration with Ruth Heidelberger, we found that the SNARE protein syntaxin 3B plays an essential role in synchronous multiquantal release at salamander rod ribbons [92]. We hypothesized that the presence of syntaxin 3B on adjoining vesicles may facilitate homotypic fusion between neighboring vesicles on the ribbon prior to their fusion with the plasma membrane. In studies on release from bipolar cells, variations in quantal amplitude have been shown to improve the coding of information about contrast [107]; multivesicular release events may play a similar role at photoreceptor synapses.

Spontaneous release events in mouse cones range widely in amplitude but with similar kinetics, akin to synchronous multiquantal events in salamander rods and cones [79]. However, multiquantal release in mouse rods is more asynchronous. When mouse rods were voltage-clamped at − 70 mV, below the activation range for Ca^{2+} channels, we observed occasional spontaneous fusion events that were relatively uniform in amplitude suggesting they arose from individual vesicles (Fig. 5). With depolarization, the rate of vesicle release increased in parallel with I_{Ca} [94]. As the membrane potential approached − 40 mV, release transitioned from unitary events to coordinated bursts of multiple vesicles (Fig. 5). These bursts typically involved the asynchronous release of 10–20 vesicles from the RRP at semi-regular intervals of roughly once per second at room temperature [94].

Absorption of a single photon hyperpolarizes mouse rods by only ~ 3.4 mV and produces an even smaller 1 mV response in primate rods [38, 188]. A 3.4 mV change in mouse rods causes ~ 20–25% reduction in I_{Ca} and a similar reduction in release [94]. One strategy that has been proposed as a means of distinguishing light-driven changes in release rate from random pauses is to release vesicles at an extremely high rate [173, 174, 234]. However, this strategy requires release rates of 80–100 v/s/ribbon, well above those found in mouse rods where release rises only to about 10–12 v/s/ribbon at the dark resting membrane potential in darkness. A second strategy is to make release more regular, and thus more predictable. This can be achieved by implementing an Erlang distribution that waits a certain number of Poisson intervals before triggering a release event [183]. This approach has been termed the “clockwork” mechanism. The sensitivity to small voltage changes and regularity of multiquantal bursts in mouse rods may improve post-synaptic detection of single photons [93]. The high levels of glutamate achieved in the cleft by release of multiple vesicles during a burst may also help to maintain high levels of glutamate in the cleft, thus keeping mGluR6 receptors close to saturation in darkness. This is important for introducing a non-linearity at the synapse whereby only larger hyperpolarizing membrane voltage changes in a rod (that are more likely to reflect genuine responses to photon absorption) will cause a sufficiently large decline in glutamate levels to generate a detectable post-synaptic response [71, 162, 181].

Non-ribbon release in rods

Unlike cones where selectively damaging ribbons abolished both fast and slow components of release equally, damaging rod ribbons by FALI preferentially reduced fast release but left the slower component largely unaffected [44]. The initial fast component of release from rods thus appears to arise from the ribbon and involves similar mechanisms as ribbon-mediated release from cones [126, 233]. The major difference in release from rods and cones is that rods are capable of release at non-ribbon sites, whereas cones are not. In both salamander and mouse rods, non-ribbon release from rods can be triggered by Ca^{2+}-induced Ca^{2+} release (CICR) from intracellular endoplasmic reticulum (ER) stores [12, 34, 202]. The Ca^{2+} released from intracellular stores in the rod terminal can help sustain release during lengthy depolarizing stimuli (e.g., in maintained darkness). Immunohistochemical staining for SERCA and labeling with ER tracker dye both showed the presence of ER in rod terminals [12, 45]. Electron micrographs also showed putative ER within 500 nm of ribbons [12] but similar structures have also been identified as endosomes [73]. The ER

forms a continuous network throughout the cell, extending from the synaptic terminal to the soma. Imaging of ER Ca^{2+} levels showed that Ca^{2+} could move within the ER between the soma and terminal compartments [45]. Cytoplasmic Ca^{2+} changes that accompany opening of Ca^{2+} channels are typically restricted to regions close to Ca^{2+} channels in the terminal and do not travel up the axon. However, CICR triggered by local Ca^{2+} changes can deplete ER stores within the terminal. These stores can then be refilled by Ca^{2+} diffusing within the ER from other parts of the rod. As Ca^{2+} ions move from the soma to the terminal to restore intraterminal ER Ca^{2+}, ER depleted in the soma can itself be refilled by the actions of SERCA and store-operated Ca^{2+} channels [119, 203, 204]. Inhibiting store-operated Ca^{2+} channels therefore has a similar inhibitory effect on release as inhibiting CICR in rods [12, 34, 202, 203]. An interesting question is whether the ability of Ca^{2+} ions to move within the ER also provides a means for intraterminal Ca^{2+} changes to influence activity in the soma and nucleus.

What is the role of CICR in release? Blocking CICR produces changes in baseline currents in bipolar and horizontal cells consistent with a reduction in basal glutamate levels in the synaptic cleft [12, 34, 121, 202, 247]. Unlike salamander cone synapses where the glutamate released from each vesicle acts independently and glutamate is rapidly removed from the cleft, glutamate levels at rod synapses rise and fall more slowly [33]. Elimination of Syt1 from mouse rods blocked fast release of the RRP but slow release evoked by long depolarizing steps, which likely reflects non-ribbon release, persisted [79]. However, the rod-driven ERG b-wave in mouse retina was almost completely abolished by elimination of Syt1 from rods suggesting that this slow, non-ribbon component of release plays at best a minor role in shaping post-synaptic light responses [79]. On the other hand, inhibiting CICR with a high concentration of ryanodine reduced bipolar and horizontal cell light responses and the ERG b-wave by 50% or more in both mouse and salamander retina [12, 34] suggesting a more significant role for non-ribbon release in shaping rod-driven light response.

Although further experiments are needed to reconcile these findings, we favor the idea that ribbon-mediated release is more important for signaling rapid light-evoked changes and non-ribbon release is more important for regulating basal levels of glutamate in the cleft. Changes in basal glutamate levels in the cleft could modulate synaptic transmission by altering the sensitivity of pre-and post-synaptic glutamate receptors. For example, non-ribbon release may help to maintain high levels of cleft glutamate needed for the non-linear thresholding mechanism in rod bipolar cells described above [71, 181]. Changes in basal glutamate could also act on presynaptic autoreceptors that may include both metabotropic and ionotropic glutamate receptors [90, 101, 116, 117]. For example, activation of mGluR8 by cleft glutamate can lead to a reduction in intracellular Ca^{2+} in rods [116, 117], providing a potential negative feedback mechanism for stabilizing Ca^{2+} levels. Resting Ca^{2+} levels in rods and cones at − 70 mV are maintained at low levels much like other neurons (ca. 100 nM) despite weak endogenous Ca^{2+} buffering in salamander rods and cones, equivalent to 50–100 μM EGTA [47, 146, 198, 203, 232].

Spontaneous release

Even at a membrane potential of − 70 mV where Ca^{2+} channels show little or no activity, individual release events can be seen in both rods and cones [52, 79, 92, 139]. Spontaneous release from cones at − 70 mV was not blocked by Co^{2+}, Cd^{2+}, or by intracellular introduction of the fast Ca^{2+} buffer, BAPTA (10 mM), indicating that it is Ca^{2+}-independent [52, 139]. In rods, the frequency of spontaneous events is reduced but not eliminated by Cd^{2+} and BAPTA suggesting the presence of both Ca^{2+}-dependent and independent events [52, 94]. Deletion of Syt1 in mouse photoreceptors elevated spontaneous release frequency in rods but not cones [79]. This increase in spontaneous release is consistent with findings in other systems where Syt1 clamps the SNARE apparatus to restrict Ca^{2+}-dependent fusion [79]. The absence of an increase in cones may be because spontaneous release in these cells is entirely Ca^{2+}-independent. In salamander rods, TIRF imaging experiments showed that spontaneous release involves both ribbon and non-ribbon sites [52]. During hibernation, ground squirrels disassemble the ribbons in their cones [178] and accompanying this change is a reduction in the size and frequency of individual spontaneous release events [144]. This suggests that, like evoked release, spontaneous release from cones involves ribbon release sites.

Rates of spontaneous release in salamander rods and cones at − 70 mV averaged 6 and 10 Hz, respectively [52]. Spontaneous release in mouse rods and cones held at − 70 mV averaged 0.9 and 5.8 Hz, respectively [79, 94]. If we normalize to the number of ribbons, spontaneous release averages ~ 0.9 Hz per ribbon in rods and 0.6–0.8 Hz per ribbon in cones of both mouse and salamander. Assuming the size of the RRP corresponds to the number of release sites along the base of the ribbon, then these numbers suggest that individual sites release vesicles spontaneously at 0.03–0.05 Hz in salamander cones, 0.04 Hz in salamander rods, and 0.01 Hz in mouse rods [19, 76, 233]. These rates are similar to those of hippocampal synapses (~ 0.01 Hz) [4, 156, 179] but tenfold higher than the frequency of ~ 0.002 Hz found at the calyx of Held [189]. It has been suggested that spontaneous release may be a means of providing an occasional “ping” signal to test whether a synaptic connection is still active. However, this function seems unnecessary at ribbon synapses where Ca^{2+}-dependent release continues ceaselessly day and night. Perhaps Ca^{2+}-independent spontaneous release is simply an unavoidable consequence of a sensitive fusion apparatus constantly poised for release.

Ribbon knockout mice

Two main genetic approaches have been used to examine the role of ribbons in release. In one set of studies, the anchoring protein bassoon was eliminated leading to photoreceptors with detached ribbons that floated within the cytoplasm. In these mice, the ERG b-wave, which reflects ON bipolar cell light responses, was severely reduced in both scotopic and photopic conditions [63]. The a-wave evoked by a flash of light (which reflects photoreceptor responses) was not reduced, showing impaired synaptic transmission from rods and cones. Whole cell recordings from cone-driven horizontal cells in mouse retina showed that after loss of bassoon, tonic glutamate release and post-synaptic light responses were both reduced. The slowing of tonic release, impaired replenishment and reduction in

the size of the RRP in bassoon knockout mice [10] are generally consistent with the view of the ribbon obtained from studies in salamander retina.

Targeting the B domain of ribeye is lethal, so ribeye knockout mice were developed by targeting the ribbon-specific A domain [141]. Ribeye knockout mice lack ribbons entirely. These mice showed impaired release from rods and rod bipolar cells and a reduction in the scotopic b-wave, similar to bassoon knockout mice [70, 76, 141]. However, unlike bassoon knockouts, the photopic b-wave reflecting cone output, was unchanged in ribeye KO mice. This was surprising given evidence from other approaches (e.g., FALI) that release from cones occurs exclusively at ribbons. Direct measurements of release from cones lacking ribbons have not yet been reported but presumably the cone is able to release vesicles at non-ribbon sites in the absence of ribbons. Despite substantial deficits in release from rods and rod bipolar cells, recordings from large ON-α ganglion cells that receive strong rod and cone inputs in ribeye KO mice showed surprisingly modest changes in light-evoked spiking, even at scotopic light intensities. Ribeye KO mice showed a decrease in contrast sensitivity, slightly longer latency responses to light increments, and slightly weaker responses to light decrements [161]. While at first glance, these results might suggest that ribbons are largely dispensable for retinal signaling, the persistence of robust light-driven activity may instead reflect the ability of retinal ganglion cells to compensate for diminished excitatory rod and cone input by reducing inhibition in the inner retina [39, 40]. However, the unexpectedly small changes in ribeye knockout mice shows that we still lack a full understanding of the roles played by photoreceptor ribbons in shaping vision.

Conclusions and future directions

Because of the large cell size and robust physiology, salamander retina has served as a valuable preparation for analyzing properties of release from rods and cones. A number of studies have also been done using the cone-dominated ground squirrel retina and recent studies have begun to analyze release from mouse retina. Conclusions about the mechanisms of release employed by rods and cones in mammalian retina are so far generally in agreement with those from amphibian retina suggesting that many of these fundamental mechanisms are highly conserved. This is consistent with the conserved nature of many other aspects of the circuitry in vertebrate retina [248]. The differences that have so far emerged appear to relate to specialized requirements of bipolar cells. For example, AMPA receptors of OFF bipolar cells in salamander do not appear to saturate during release unlike those of ground squirrel [77, 163]. Amphibian retinas lack the specialized rod bipolar cell found in mammals and the input into these cells from mouse rods involves coordinated bursts of vesicle release that are not seen in salamander rods [94].

Many questions still remain concerning rod and cone synapses. For example, along with a general understanding of the role of ribbons in release, what are the specific roles of the enzymatic domains of ribeye? What are the roles played by ribbon-specific variants of proteins such as syntaxin 3B and complexins 3 and 4? How does the presence of an arciform density shape Ca^{2+} nanodomains and the properties of release? How are vesicles primed for release at rod and cone ribbons if they do not use Rim2 and Munc13? What is the molecular make-up of the tethers? What are the mechanisms of fast endocytosis at rods and

cones? Do they incorporate kiss-and-run? What role, if any, does spontaneous release play at these synapses? Is the unusual Ca^{2+}-sensitivity of amphibian rods and cones retained at mammalian synapses that use Syt1? If so, what accounts for this difference? What is the impact of synchronous and sequential multivesicular release on coding of light responses at rod and cone synapses? What is the role of non-ribbon release in rods? What are the Ca^{2+} sensors that regulate non-ribbon release in rods? Why are rods but not cones capable of non-ribbon release?

In addition to answering these and other questions concerning release at rod and cone synapses, a better understanding of these mechanisms provides opportunities for exploring disease-related changes. In the auditory system, various cochlear synaptopathies have been identified as contributing to hearing loss [130]. Synaptopathies affecting photoreceptors also contribute to vision loss [164]. The best recognized examples are the mutations in photoreceptor Ca^{2+} channels and associated proteins that can cause CSNB [251]. Mutations in other proteins found at photoreceptor synapses including Rim, Tulp1, and dystrophin are also associated with retinal degeneration [18, 42, 84]. In addition, retinal diseases that do not arise from specific mutations in synaptic proteins may also involve synaptic changes in photoreceptors. For example, changes in the ERG suggest impaired transmission from rods is present early in diabetes [165]. And in patients with age-related macular degeneration, photoreceptors show diminished expression of synaptic proteins, loss of ribbons, and altered synaptic structure [109]. Similar synaptic deficits have been seen in mouse models of age-related macular degeneration [254] and choroidal neovascularization [37]. We also observed a decrease in synaptic release from photoreceptors in a model of Stargardt's disease [25]. Further study of photoreceptor synapses are likely to reveal other synaptopathies that contribute to vision loss.

Acknowledgments

I also thank many colleagues and collaborators for their contributions.

Funding

Research from my laboratory described in this review was supported largely by NIH grant EY10542 along with grants from Research to Prevent Blindness.

References

1. Abe H, Yamamoto TY (1984) Diurnal changes in synaptic ribbons of rod cells of the turtle. J Ultrastruct Res 86:246–251. 10.1016/s0022-5320(84)90104-7 [PubMed: 6544862]
2. Adly MA, Spiwoks-Becker I, Vollrath L (1999) Ultrastructural changes of photoreceptor synaptic ribbons in relation to time of day and illumination. Invest Ophthalmol Vis Sci 40:2165–2172 [PubMed: 10476779]
3. Ahnelt P, Kolb H (1994) Horizontal cells and cone photoreceptors in human retina: a golgi-electron microscopic study of spectral connectivity. J Comp Neurol 343:406–427. 10.1002/cne.903430306 [PubMed: 8027450]
4. Arancillo M, Min SW, Gerber S, Munster-Wandowski A, Wu YJ, Herman M, Trimbuch T, Rah JC, Ahnert-Hilger G, Riedel D, Sudhof TC, Rosenmund C (2013) Titration of Syntaxin1 in mammalian synapses reveals multiple roles in vesicle docking, priming, and release probability. J Neurosci 33:16698–16714. 10.1523/JNEUROSCI.0187-1.2013 [PubMed: 24133272]

5. Armstrong-Gold CE, Rieke F (2003) Bandpass filtering at the rod to second-order cell synapse in salamander (*Ambystoma tigrinum*) retina. J Neurosci 23:3796–3806. 10.1523/jneurosci.23-09-03796.2003 [PubMed: 12736350]
6. Arriza JL, Eliasof S, Kavanaugh MP, Amara SG (1997) Excitatory amino acid transporter 5, a retinal glutamate transporter coupled to a chloride conductance. Proc Natl Acad Sci U S A 94:4155–4160. 10.1073/pnas.94.8.4155 [PubMed: 9108121]
7. Arshavsky VY, Burns ME (2012) Photoreceptor signaling: supporting vision across a wide range of light intensities. J Biol Chem 287:1620–1626. 10.1074/jbc.R111.305243 [PubMed: 22074925]
8. Attwell D, Borges S, Wu SM, Wilson M (1987) Signal clipping by the rod output synapse. Nature 328:522–524. 10.1038/328522a0 [PubMed: 3039370]
9. Babai N, Bartoletti TM, Thoreson WB (2010) Calcium regulates vesicle replenishment at the cone ribbon synapse. J Neurosci 30:15866–15877. 10.1523/JNEUROSCI.2891-10.2010 [PubMed: 21106825]
10. Babai N, Gierke K, Muller T, Regus-Leidig H, Brandstatter JH, Feigenspan A (2019) Signal transmission at invaginating cone photoreceptor synaptic contacts following deletion of the presynaptic cytomatrix protein Bassoon in mouse retina. Acta Physiol (Oxf) 226:e13241. 10.1111/apha.13241 [PubMed: 30554473]
11. Babai N, Kanevsky N, Dascal N, Rozanski GJ, Singh DP, Fatma N, Thoreson WB (2010) Anion-sensitive regions of L-type CaV1.2 calcium channels expressed in HEK293 cells. PLoS ONE 5:e8602. 10.1371/journal.pone0008602 [PubMed: 20066046]
12. Babai N, Morgans CW, Thoreson WB (2010) Calcium-induced calcium release contributes to synaptic release from mouse rod photoreceptors. Neuroscience 165:1447–1456. 10.1016/j.neuroscience.2009.11.032 [PubMed: 19932743]
13. Babai N, Sendelbeck A, Regus-Leidig H, Fuchs M, Mertins J, Reim K, Brose N, Feigenspan A, Brandstatter JH (2016) Functional roles of complexin 3 and complexin 4 at mouse photoreceptor ribbon synapses. J Neurosci 36:6651–6667. 10.1523/JNEURSCI.4335-15.2016 [PubMed: 27335398]
14. Babai N, Thoreson WB (2009) Horizontal cell feedback regulates calcium currents and intracellular calcium levels in rod photoreceptors of salamander and mouse retina. J Physiol 587:2353–2364. 10.1113/jphysiol.2009.169656 [PubMed: 19332495]
15. Ball SL, Powers PA, Shin HS, Morgans CW, Peachey NS, Gregg RG (2002) Role of the beta(2) subunit of voltage-dependent calcium channels in the retinal outer plexiform layer. Invest Ophthalmol Vis Sci 43:1595–1603 [PubMed: 11980879]
16. Barnes S, Bui Q (1991) Modulation of calcium-activated chloride current via pH-induced changes of calcium channel properties in cone photoreceptors. J Neurosci 11:4015–4023. 10.1523/JNEUROSCI.11-12-04015.1991 [PubMed: 1660538]
17. Barnes S, Merchant V, Mahmud F (1993) Modulation of transmission gain by protons at the photoreceptor output synapse. Proc Natl Acad Sci U S A 90:10081–10085. 10.1073/pnas.90.21.10081 [PubMed: 7694280]
18. Barragan I, Marcos I, Borrego S, Antinolo G (2005) Molecular analysis of RIM1 in autosomal recessive *Retinitis pigmentosa*. Ophthalmic Res 37:89–93. 10.1159/000084250 [PubMed: 15746564]
19. Bartoletti TM, Babai N, Thoreson WB (2010) Vesicle pool size at the salamander cone ribbon synapse. J Neurophysiol 103:419–423. 10.1152/jn.00718.2009 [PubMed: 19923246]
20. Bartoletti TM, Jackman SL, Babai N, Mercer AJ, Kramer RH, Thoreson WB (2011) Release from the cone ribbon synapse under bright light conditions can be controlled by the opening of only a few Ca(2+) channels. J Neurophysiol 106:2922–2935. 10.1152/jn.00634.2011 [PubMed: 21880934]
21. Bartoletti TM, Thoreson WB (2011) Quantal amplitude at the cone ribbon synapse can be adjusted by changes in cytosolic glutamate. Mol Vis 17:920–931 [PubMed: 21541265]
22. Baumann L, Gerstner A, Zong X, Biel M, Wahl-Schott C (2004) Functional characterization of the L-type Ca^{2+} channel Cav1.4alpha1 from mouse retina. Invest Ophthalmol Vis Sci 45:708–713. 10.1167/iovs.03-0937 [PubMed: 14744918]

23. Baylor DA, Fuortes MG, O'Bryan PM (1971) Lateral interaction between vertebrate photoreceptors. Vision Res 11:1195–1196. 10.1016/0042-6989(71)90134-9
24. Behrens C, Schubert T, Haverkamp S, Euler T, Berens P (2016) Connectivity map of bipolar cells and photoreceptors in the mouse retina. Elife 5. 10.7554/eLife.20041
25. Bennett LD, Hopiavuori BR, Brush RS, Chan M, Van Hook MJ, Thoreson WB, Anderson RE (2014) Examination of VLC-PUFA-deficient photoreceptor terminals. Invest Ophthalmol Vis Sci 55:4063–4072. 10.1167/iovs.14-13997 [PubMed: 24764063]
26. Berntson A, Taylor WR (2003) The unitary event amplitude of mouse retinal on-cone bipolar cells. Vis Neurosci 20:621–626. 10.1017/s0952523803206040 [PubMed: 15088715]
27. Berntson AK, Morgans CW (2003) Distribution of the presynaptic calcium sensors, synaptotagmin I/II and synaptotagmin III, in the goldfish and rodent retinas. J Vis 3:274–280. 10.1167/3.4.3 [PubMed: 12803536]
28. Borst JG, Sakmann B (1999) Depletion of calcium in the synaptic cleft of a calyx-type synapse in the rat brainstem. J Physiol 521(Pt 1):123–133. 10.1111/j.1469-7793.1999.00123.x [PubMed: 10562339]
29. Bowen RW, Pokorny J, Smith VC (1989) Sawtooth contrast sensitivity: decrements have the edge. Vision Res 29:1501–1509. 10.1016/0042-6989(89)90134-x [PubMed: 2635476]
30. Brandstatter JH, Fletcher EL, Garner CC, Gundelfinger ED, Wassle H (1999) Differential expression of the presynaptic cytomatrix protein bassoon among ribbon synapses in the mammalian retina. Eur J Neurosci 11:3683–3693. 10.1046/j.1460-9568.1999.00793.x [PubMed: 10564375]
31. Burns ME, Baylor DA (2001) Activation, deactivation, and adaptation in vertebrate photoreceptor cells. Annu Rev Neurosci 24:779–805. 10.1146/annurev.neuro.24.1.779 [PubMed: 11520918]
32. Burtscher V, Schicker K, Novikova E, Pohn B, Stockner T, Kugler C, Singh A, Zeitz C, Lancelot ME, Audo I, Leroy BP, Freissmuth M, Herzig S, Matthes J, Koschak A (2014) Spectrum of Cav1.4 dysfunction in congenital stationary night blindness type 2. Biochim Biophys Acta 1838:2053–2065. 10.1016/j.bbamem.2014.04.023 [PubMed: 24796500]
33. Cadetti L, Bartoletti TM, Thoreson WB (2008) Quantal mEPSCs and residual glutamate: how horizontal cell responses are shaped at the photoreceptor ribbon synapse. Eur J Neurosci 27:2575–2586. 10.1111/j.1460-9568.2008.06226.x [PubMed: 18547244]
34. Cadetti L, Bryson EJ, Ciccone CA, Rabl K, Thoreson WB (2006) Calcium-induced calcium release in rod photoreceptor terminals boosts synaptic transmission during maintained depolarization. Eur J Neurosci 23:2983–2990. 10.1111/j.1460-9568.2006.04845.x [PubMed: 16819987]
35. Cadetti L, Thoreson WB (2006) Feedback effects of horizontal cell membrane potential on cone calcium currents studied with simultaneous recordings. J Neurophysiol 95:1992–1995. 10.1152/jn.01042.2005 [PubMed: 16371457]
36. Cadetti L, Tranchina D, Thoreson WB (2005) A comparison of release kinetics and glutamate receptor properties in shaping rod-cone differences in EPSC kinetics in the salamander retina. J Physiol 569:773–788. 10.1113/jphysiol.2005.096545 [PubMed: 16223761]
37. Caicedo A, Espinosa-Heidmann DG, Hamasaki D, Pina Y, Cousins SW (2005) Photoreceptor synapses degenerate early in experimental choroidal neovascularization. J Comp Neurol 483:263–277. 10.1002/cne.20413 [PubMed: 15682400]
38. Cangiano L, Asteriti S, Cervetto L, Gargini C (2012) The photovoltage of rods and cones in the dark-adapted mouse retina. J Physiol 590:3841–3855. 10.1113/jphysiol.2011.226878 [PubMed: 22641773]
39. Care RA, Anastassov IA, Kastner DB, Kuo YM, Della Santina L, Dunn FA (2020) Mature retina compensates functionally for partial loss of rod photoreceptors. Cell Rep 31:107730. 10.1016/j.celrep.2020.107730 [PubMed: 32521255]
40. Care RA, Kastner DB, De la Huerta I, Pan S, Khoche A, Della Santina L, Gamlin C, Santo Tomas C, Ngo J, Chen A, Kuo YM, Ou Y, Dunn FA (2019) Partial cone loss triggers synapse-specific remodeling and spatial receptive field rearrangements in a mature retinal circuit. Cell Rep 27(2171–2183):e2175. 10.1016/j.celrep.2019.04.065

41. Carter-Dawson LD, LaVail MM (1979) Rods and cones in the mouse retina. I. Structural analysis using light and electron microscopy. J Comp Neurol 188:245–262. 10.1002/cne.901880204 [PubMed: 500858]
42. Catalani E, Bongiorni S, Taddei AR, Mezzetti M, Silvestri F, Coazzoli M, Zecchini S, Giovarelli M, Perrotta C, De Palma C, Clementi E, Ceci M, Prantera G, Cervia D (2020) Defects of full-length dystrophin trigger retinal neuron damage and synapse alterations by disrupting functional autophagy. Cell Mol Life Sci. 10.1007/s00018-020-03598-5
43. Chapot CA, Behrens C, Rogerson LE, Baden T, Pop S, Berens P, Euler T, Schubert T (2017) Local signals in mouse horizontal cell dendrites. Curr Biol 27:3603–3615 e3605. 10.1016/j.cub.2017.10.050 [PubMed: 29174891]
44. Chen M, Krizaj D, Thoreson WB (2014) Intracellular calcium stores drive slow non-ribbon vesicle release from rod photoreceptors. Front Cell Neurosci 8:20. 10.3389/fncel.2014.00020 [PubMed: 24550779]
45. Chen M, Van Hook MJ, Thoreson WB (2015) Ca^{2+} diffusion through endoplasmic reticulum supports elevated intraterminal Ca^{2+} levels needed to sustain synaptic release from rods in darkness. J Neurosci 35:11364–11373. 10.1523/JNEUROSCI.0754-15.2015 [PubMed: 26269643]
46. Chen M, Van Hook MJ, Zenisek D, Thoreson WB (2013) Properties of ribbon and non-ribbon release from rod photoreceptors revealed by visualizing individual synaptic vesicles. J Neurosci 33:2071–2086. 10.1523/JNEUROSCI.3426-12.2013 [PubMed: 23365244]
47. Choi SY, Jackman S, Thoreson WB, Kramer RH (2008) Light regulation of Ca^{2+} in the cone photoreceptor synaptic terminal. Vis Neurosci 25:693–700. 10.1017/s0952523808080814 [PubMed: 19112656]
48. Chun MH, Grunert U, Martin PR, Wassle H (1996) The synaptic complex of cones in the fovea and in the periphery of the macaque monkey retina. Vision Res 36:3383–3395. 10.1016/0042-6989(95)00334-7 [PubMed: 8977005]
49. Cooper B, Hemmerlein M, Ammermuller J, Imig C, Reim K, Lipstein N, Kalla S, Kawabe H, Brose N, Brandstatter JH, Varoqueaux F (2012) Munc13-independent vesicle priming at mouse photoreceptor ribbon synapses. J Neurosci 32:8040–8052. 10.1523/JNEUROSCI.4240-11.2012 [PubMed: 22674279]
50. Corey DP, Dubinsky JM, Schwartz EA (1984) The calcium current in inner segments of rods from the salamander (Ambystoma tigrinum) retina. J Physiol 354:557–575. 10.1113/jphysiol.1984.sp015393 [PubMed: 6090654]
51. Cork KM, Thoreson WB (2014) Rapid kinetics of endocytosis at rod photoreceptor synapses depends upon endocytic load and calcium. Vis Neurosci 31:227–235. 10.1017/S095252381400011X [PubMed: 24735554]
52. Cork KM, Van Hook MJ, Thoreson WB (2016) Mechanisms, pools, and sites of spontaneous vesicle release at synapses of rod and cone photoreceptors. Eur J Neurosci 44:2015–2027. 10.1111/ejn.13288 [PubMed: 27255664]
53. Curtis L, Datta P, Liu X, Bogdanova N, Heidelberger R, Janz R (2010) Syntaxin 3B is essential for the exocytosis of synaptic vesicles in ribbon synapses of the retina. Neuroscience 166:832–841. 10.1016/j.neuroscience.2009.12.075 [PubMed: 20060037]
54. Datta P, Gilliam J, Thoreson WB, Janz R, Heidelberger R (2017) Two pools of vesicles associated with synaptic ribbons are molecularly prepared for release. Biophys J 113:2281–2298. 10.1016/j.bpj.2017.08.012 [PubMed: 28863864]
55. Dauner K, Mobus C, Frings S, Mohrlen F (2013) Targeted expression of anoctamin calcium-activated chloride channels in rod photoreceptor terminals of the rodent retina. Invest Ophthalmol Vis Sci 54:3126–3136. 10.1167/iovs.13-11711 [PubMed: 23557741]
56. Davies A, Kadurin I, Alvarez-Laviada A, Douglas L, Nieto-Rostro M, Bauer CS, Pratt WS, Dolphin AC (2010) The alpha2delta subunits of voltage-gated calcium channels form GPI-anchored proteins, a posttranslational modification essential for function. Proc Natl Acad Sci U S A 107:1654–1659. 10.1073/pnas.0908735107 [PubMed: 20080692]
57. De Robertis E, Franchi CM (1956) Electron microscope observations on synaptic vesicles in synapses of the retinal rods and cones. J Biophys Biochem Cytol 2:307–318. 10.1083/jcb.2.3.307 [PubMed: 13331963]

58. Deguchi-Tawarada M, Inoue E, Takao-Rikitsu E, Inoue M, Kitajima I, Ohtsuka T, Takai Y (2006) Active zone protein CAST is a component of conventional and ribbon synapses in mouse retina. J Comp Neurol 495:480–496. 10.1002/cne.20893 [PubMed: 16485285]
59. Dembla E, Dembla M, Maxeiner S, Schmitz F (2020) Synaptic ribbons foster active zone stability and illumination-dependent active zone enrichment of RIM2 and Cav1.4 in photoreceptor synapses. Sci Rep 10:5957. 10.1038/s41598-020-62734-0 [PubMed: 32249787]
60. DeVries SH (2000) Bipolar cells use kainate and AMPA receptors to filter visual information into separate channels. Neuron 28:847–856. 10.1016/s0896-6273(00)00158-6 [PubMed: 11163271]
61. DeVries SH (2001) Exocytosed protons feedback to suppress the Ca^{2+} current in mammalian cone photoreceptors. Neuron 32:1107–1117. 10.1016/s0896-6273(01)00535-9 [PubMed: 11754841]
62. DeVries SH, Li W, Saszik S (2006) Parallel processing in two transmitter microenvironments at the cone photoreceptor synapse. Neuron 50:735–748. 10.1016/j.neuron.2006.04.034 [PubMed: 16731512]
63. Dick O, tom Dieck SS, Altrock WD, Ammermuller J, Weiler R, Garner GC, Gundelfinger ED, Brandstatter JH (2003) The presynaptic active zone protein bassoon is essential for photoreceptor ribbon synapse formation in the retina. Neuron 37:775–786. 10.1016/s0896-6273(03)00086-2 [PubMed: 12628168]
64. Doering CJ, Hamid J, Simms B, McRory JE, Zamponi GW (2005) Cav1.4 encodes a calcium channel with low open probability and unitary conductance. Biophys J 89:3042–3048. 10.1529/biophysj.105.067124 [PubMed: 16085774]
65. Dolphin AC, Lee A (2020) Presynaptic calcium channels: specialized control of synaptic neurotransmitter release. Nat Rev Neurosci 21:213–229. 10.1038/s41583-020-0278-2 [PubMed: 32161339]
66. Duncan G, Rabl K, Gemp I, Heidelberger R, Thoreson WB (2010) Quantitative analysis of synaptic release at the photoreceptor synapse. Biophys J 98:2102–2110. 10.1016/j.bpj.2010.02.003 [PubMed: 20483317]
67. Eliasof S, Jahr CE (1996) Retinal glial cell glutamate transporter is coupled to an anionic conductance. Proc Natl Acad Sci U S A 93:4153–4158. 10.1073/pnas.93.9.4153 [PubMed: 8633032]
68. Euler T, Haverkamp S, Schubert T, Baden T (2014) Retinal bipolar cells: elementary building blocks of vision. Nat Rev Neurosci 15:507–519. 10.1038/nrn3783 [PubMed: 25158357]
69. Fain GL, Hardie R, Laughlin SB (2010) Phototransduction and the evolution of photoreceptors. Curr Biol 20:R114–124. 10.1016/j.cub.2009.12.006 [PubMed: 20144772]
70. Fairless R, Williams SK, Katiyar R, Maxeiner S, Schmitz F, Diem R (2020) ERG responses in mice with deletion of the synaptic ribbon component RIBEYE. Invest Ophthalmol Vis Sci 61:37. 10.1167/iovs.61.5.37
71. Field GD, Rieke F (2002) Nonlinear signal transfer from mouse rods to bipolar cells and implications for visual sensitivity. Neuron 34:773–785. 10.1016/s0896-6273(02)00700-6 [PubMed: 12062023]
72. Fox MA, Sanes JR (2007) Synaptotagmin I and II are present in distinct subsets of central synapses. J Comp Neurol 503:280–296. 10.1002/cne.21381 [PubMed: 17492637]
73. Fuchs M, Brandstatter JH, Regus-Leidig H (2014) Evidence for a Clathrin-independent mode of endocytosis at a continuously active sensory synapse. Front Cell Neurosci 8:60. 10.3389/fncel.2014.00060 [PubMed: 24616664]
74. Giarmarco MM, Cleghorn WM, Sloat SR, Hurley JB, Brockerhoff SE (2017) Mitochondria maintain distinct Ca(2+) pools in cone photoreceptors. J Neurosci 37:2061–2072. 10.1523/JNEUROSCI.2689-16.2017 [PubMed: 28115482]
75. Grabner CP, Gandini MA, Rehak R, Le Y, Zamponi GW, Schmitz F (2015) RIM1/2-mediated facilitation of Cav1.4 channel opening is required for Ca^{2+}-stimulated release in mouse rod photoreceptors. J Neurosci 35:13133–13147. 10.1523/JNEUROSCI.0658-15.2015 [PubMed: 26400943]
76. Grabner CP, Moser T (2020) The mammalian rod synaptic ribbon is essential for Cav channel facilitation and ultrafast fusion of the readily releasable pool of vesicles. bioRxiv 10.1101/2020.10.12.336503

77. Grabner CP, Ratliff CP, Light AC, DeVries SH (2016) Mechanism of high-frequency signaling at a depressing ribbon synapse. Neuron 91:133–145. 10.1016/j.neuron.2016.05.019 [PubMed: 27292536]
78. Grant GB, Werblin FS (1996) A glutamate-elicited chloride current with transporter-like properties in rod photoreceptors of the tiger salamander. Vis Neurosci 13:135–144. 10.1017/s0952523800007185 [PubMed: 8730995]
79. Grassmeyer JJ, Cahill AL, Hays CL, Barta C, Quadros RM, Gurumurthy CB, Thoreson WB (2019) Ca(2+) sensor synaptotagmin-1 mediates exocytosis in mammalian photoreceptors. Elife 8. 10.7554/eLife.45946
80. Grassmeyer JJ, Thoreson WB (2017) Synaptic ribbon active zones in cone photoreceptors operate independently from one another. Front Cell Neurosci 11:198. 10.3389/fncel.2017.00198 [PubMed: 28744203]
81. Gray EG, Pease HL (1971) On understanding the organisation of the retinal receptor synapses. Brain Res 35:1–15. 10.1016/0006-8993(71)90591-9 [PubMed: 5134225]
82. Graydon CW, Cho S, Li GL, Kachar B, von Gersdorff H (2011) Sharp Ca(2)(+) nanodomains beneath the ribbon promote highly synchronous multivesicular release at hair cell synapses. J Neurosci 31:16637–16650. 10.1523/JNEUROSCI.1866-11.2011 [PubMed: 22090491]
83. Graydon CW, Zhang J, Oesch NW, Sousa AA, Leapman RD, Diamond JS (2014) Passive diffusion as a mechanism underlying ribbon synapse vesicle release and resupply. J Neurosci 34:8948–8962. 10.1523/JNEUROSCI.1022-14.2014 [PubMed: 24990916]
84. Grossman GH, Pauer GJ, Narendra U, Hagstrom SA (2010) Tubby-like protein 1 (Tulp1) is required for normal photoreceptor synaptic development. Adv Exp Med Biol 664:89–96. 10.1007/978-1-4419-1399-9_11 [PubMed: 20238006]
85. Grunert U, Martin PR (1991) Rod bipolar cells in the macaque monkey retina: immunoreactivity and connectivity. J Neurosci 11:2742–2758. 10.1523/JNEUROSCI.11-09-02742.1991 [PubMed: 1715391]
86. Haeseleer F, Imanishi Y, Maeda T, Possin DE, Maeda A, Lee A, Rieke F, Palczewski K (2004) Essential role of Ca^{2+}-binding protein 4, a Cav1.4 channel regulator, in photoreceptor synaptic function. Nat Neurosci 7:1079–1087. 10.1038/nn1320 [PubMed: 15452577]
87. Haeseleer F, Williams B, Lee A (2016) Characterization of C-terminal splice variants of Cav1.4 Ca^{2+} channels in human retina. J Biol Chem 291:15663–15673. 10.1074/jbc.M116.731737 [PubMed: 27226626]
88. Hagiwara A, Kitahara Y, Grabner CP, Vogl C, Abe M, Kitta R, Ohta K, Nakamura K, Sakimura K, Moser T, Nishi A, Ohtsuka T (2018) Cytomatrix proteins CAST and ELKS regulate retinal photoreceptor development and maintenance. J Cell Biol 217:3993–4006. 10.1083/jcb201704076 [PubMed: 30190286]
89. Hasegawa J, Obara T, Tanaka K, Tachibana M (2006) High-density presynaptic transporters are required for glutamate removal from the first visual synapse. Neuron 50:63–74. 10.1016/j.neuron.2006.02.022 [PubMed: 16600856]
90. Haumann I, Junghans D, Anstotz M, Frotscher M (2017) Presynaptic localization of GluK5 in rod photoreceptors suggests a novel function of high affinity glutamate receptors in the mammalian retina. PLoS ONE 12:e0172967. 10.1371/journal.pone.0172967 [PubMed: 28235022]
91. Haverkamp S, Grunert U, Wassle H (2000) The cone pedicle, a complex synapse in the retina. Neuron 27:85–95. 10.1016/s0896-6273(00)00011-8 [PubMed: 10939333]
92. Hays CL, Grassmeyer JJ, Wen X, Janz R, Heidelberger R, Thoreson WB (2020) Simultaneous release of multiple vesicles from rods involves synaptic ribbons and syntaxin 3B. Biophys J 118:967–979. 10.1016/j.bpj.2019.10.006 [PubMed: 31653448]
93. Hays CL SA, Field GD, Thoreson WB (2021) Properties of multi-vesicular release from rod photoreceptors support transmission of single photon responses. bioRxiv 2021.02.01.429179. 10.1101/2021.02.01.429179
94. Hays CL, Sladek AL, Thoreson WB (2020) Resting and stimulated mouse rod photoreceptors show distinct patterns of vesicle release at ribbon synapses. J Gen Physiol 152:e202012716. 10.1085/jgp.202012716 [PubMed: 33175961]

95. Heidelberger R, Sterling P, Matthews G (2002) Roles of ATP in depletion and replenishment of the releasable pool of synaptic vesicles. J Neurophysiol 88:98–106. 10.1152/jn.2002.88.1.98 [PubMed: 12091535]

96. Heidelberger R, Wang MM, Sherry DM (2003) Differential distribution of synaptotagmin immunoreactivity among synapses in the goldfish, salamander, and mouse retina. Vis Neurosci 20:37–49. 10.1017/s095252380320105x [PubMed: 12699082]

97. Hirasawa H, Kaneko A (2003) pH changes in the invaginating synaptic cleft mediate feedback from horizontal cells to cone photoreceptors by modulating Ca^{2+} channels. J Gen Physiol 122:657–671. 10.1085/jgp.200308863 [PubMed: 14610018]

98. Holmberg K, Ohman P (1976) Fine structure of retinal synaptic organelles in lamprey and hagfish photoreceptors. Vision Res 16:237–239. 10.1016/0042-6989(76)90105-x [PubMed: 1266067]

99. Holzhausen LC, Lewis AA, Cheong KK, Brockerhoff SE (2009) Differential role for synaptojanin 1 in rod and cone photoreceptors. J Comp Neurol 517:633–644. 10.1002/cne.22176 [PubMed: 19827152]

100. Hori T, Takahashi T (2012) Kinetics of synaptic vesicle refilling with neurotransmitter glutamate. Neuron 76:511–517. 10.1016/j.neuron.2012.08.013 [PubMed: 23141063]

101. Hosoi N, Arai I, Tachibana M (2005) Group III metabotropic glutamate receptors and exocytosed protons inhibit L-type calcium currents in cones but not in rods. J Neurosci 25:4062–4072. 10.1523/JNEUROSCI.2735-04.2005 [PubMed: 15843608]

102. Hurley JB, Lindsay KJ, Du J (2015) Glucose, lactate, and shuttling of metabolites in vertebrate retinas. J Neurosci Res 93:1079–1092. 10.1002/jnr.23583 [PubMed: 25801286]

103. Iijima T, Ciani S, Hagiwara S (1986) Effects of the external pH on Ca channels: experimental studies and theoretical considerations using a two-site, two-ion model. Proc Natl Acad Sci U S A 83:654–658. 10.1073/pnas.83.3.654 [PubMed: 2418439]

104. Ingram NT, Fain GL, Sampath AP (2020) Elevated energy requirement of cone photoreceptors. Proc Natl Acad Sci U S A 117:19599–19603. 10.1073/pnas.2001776117 [PubMed: 32719136]

105. Innocenti B, Heidelberger R (2008) Mechanisms contributing to tonic release at the cone photoreceptor ribbon synapse. J Neurophysiol 99:25–36. 10.1152/jn.00737.2007 [PubMed: 17989244]

106. Jackman SL, Choi SY, Thoreson WB, Rabl K, Bartoletti TM, Kramer RH (2009) Role of the synaptic ribbon in transmitting the cone light response. Nat Neurosci 12:303–310. 10.1038/nn.2267 [PubMed: 19219039]

107. James B, Darnet L, Moya-Diaz J, Seibel SH, Lagnado L (2019) An amplitude code transmits information at a visual synapse. Nat Neurosci 22:1140–1147. 10.1038/s41593-019-0403-6 [PubMed: 31110322]

108. Jimeno D, Feiner L, Lillo C, Teofilo K, Goldstein LS, Pierce EA, Williams DS (2006) Analysis of kinesin-2 function in photoreceptor cells using synchronous Cre-loxP knockout of Kif3a with RHO-Cre. Invest Ophthalmol Vis Sci 47:5039–5046. 10.1167/iovs.06-0032 [PubMed: 17065525]

109. Johnson PT, Brown MN, Pulliam BC, Anderson DH, Johnson LV (2005) Synaptic pathology, altered gene expression, and degeneration in photoreceptors impacted by drusen. Invest Ophthalmol Vis Sci 46:4788–4795. 10.1167/iovs.05-0767 [PubMed: 16303980]

110. Joselevitch C, Zenisek D (2020) Direct observation of vesicle transport on the synaptic ribbon provides evidence that vesicles are mobilized and prepared rapidly for release. J Neurosci 40:7390–7404. 10.1523/JNEUROSCI.0605-20.2020 [PubMed: 32847965]

111. Kantardzhieva A, Peppi M, Lane WS, Sewell WF (2012) Protein composition of immunoprecipitated synaptic ribbons. J Proteome Res 11:1163–1174. 10.1021/pr2008972 [PubMed: 22103298]

112. Kerov V, Laird JG, Joiner ML, Knecht S, Soh D, Hagen J, Gardner SH, Gutierrez W, Yoshimatsu T, Bhattarai S, Puthussery T, Artemyev NO, Drack AV, Wong RO, Baker SA, Lee A (2018) alpha2delta-4 is required for the molecular and structural organization of rod and cone photoreceptor synapses. J Neurosci 38:6145–6160. 10.1523/JNEUROSCI.3818-16.2018 [PubMed: 29875267]

113. Kits KS, Mansvelder HD (2000) Regulation of exocytosis in neuroendocrine cells: spatial organization of channels and vesicles, stimulus-secretion coupling, calcium buffers and

modulation. Brain Res Brain Res Rev 33:78–94. 10.1016/s0165-0173(00)00023-0 [PubMed: 10967354]

114. Kolb H (1970) Organization of the outer plexiform layer of the primate retina: electron microscopy of Golgi-impregnated cells. Philos Trans R Soc Lond B Biol Sci 258:261–283. 10.1098/rstb.1970.0036 [PubMed: 22408829]
115. Koschak A, Reimer D, Walter D, Hoda JC, Heinzle T, Grabner M, Striessnig J (2003) Cav1.4alpha1 subunits can form slowly inactivating dihydropyridine-sensitive L-type Ca^{2+} channels lacking Ca^{2+}-dependent inactivation. J Neurosci 23:6041–6049. 10.1523/JNEUROSCI.23-14-06041.2003 [PubMed: 12853422]
116. Koulen P, Brandstatter JH (2002) Pre-and postsynaptic sites of action of mGluR8a in the mammalian retina. Invest Ophthalmol Vis Sci 43:1933–1940 [PubMed: 12037002]
117. Koulen P, Kuhn R, Wassle H, Brandstatter JH (1999) Modulation of the intracellular calcium concentration in photoreceptor terminals by a presynaptic metabotropic glutamate receptor. Proc Natl Acad Sci U S A 96:9909–9914. 10.1073/pnas.96.17.9909 [PubMed: 10449793]
118. Kreft M, Krizaj D, Grilc S, Zorec R (2003) Properties of exocytotic response in vertebrate photoreceptors. J Neurophysiol 90:218–225. 10.1152/jn.01025.2002 [PubMed: 12660355]
119. Krizaj D (2012) Calcium stores in vertebrate photoreceptors. Adv Exp Med Biol 740:873–889. 10.1007/978-94-007-2888-2_39 [PubMed: 22453974]
120. Krizaj D, Copenhagen DR (1998) Compartmentalization of calcium extrusion mechanisms in the outer and inner segments of photoreceptors. Neuron 21:249–256. 10.1016/s0896-6273(00)80531-0 [PubMed: 9697868]
121. Krizaj D, Lai FA, Copenhagen DR (2003) Ryanodine stores and calcium regulation in the inner segments of salamander rods and cones. J Physiol 547:761–774. 10.1113/jphysiol.2002.035683 [PubMed: 12562925]
122. Lasansky A (1973) Organization of the outer synaptic layer in the retina of the larval tiger salamander. Philos Trans R Soc Lond B Biol Sci 265:471–489. 10.1098/rstb.1973.0033 [PubMed: 4147132]
123. Lasansky A (1978) Contacts between receptors and electrophysiologically identified neurones in the retina of the larval tiger salamander. J Physiol 285:531–542. 10.1113/jphysiol.1978.sp012587 [PubMed: 217992]
124. Lee A, Wang S, Williams B, Hagen J, Scheetz TE, Haeseleer F (2015) Characterization of Cav1.4 complexes (alpha11.4, beta2, and alpha2delta4) in HEK293T cells and in the retina. J Biol Chem 290:1505–1521. 10.1074/jbc.M114.607465 [PubMed: 25468907]
125. Li S, Mitchell J, Briggs DJ, Young JK, Long SS, Fuerst PG (2016) Morphological diversity of the rod spherule: a study of serially reconstructed electron micrographs. PLoS ONE 11:e0150024. 10.1371/journal.pone.0150024 [PubMed: 26930660]
126. Li W, Chen S, DeVries SH (2010) A fast rod photoreceptor signaling pathway in the mammalian retina. Nat Neurosci 13:414–416. 10.1038/nn.2507 [PubMed: 20190742]
127. Li W, DeVries SH (2006) Bipolar cell pathways for color and luminance vision in a dichromatic mammalian retina. Nat Neurosci 9:669–675. 10.1038/nn1686 [PubMed: 16617341]
128. Li W, Keung JW, Massey SC (2004) Direct synaptic connections between rods and OFF cone bipolar cells in the rabbit retina. J Comp Neurol 474:1–12. 10.1002/cne.20075 [PubMed: 15156575]
129. Libby RT, Lillo C, Kitamoto J, Williams DS, Steel KP (2004) Myosin Va is required for normal photoreceptor synaptic activity. J Cell Sci 117:4509–4515. 10.1242/jcs.01316 [PubMed: 15316067]
130. Liberman MC, Kujawa SG (2017) Cochlear synaptopathy in acquired sensorineural hearing loss: manifestations and mechanisms. Hear Res 349:138–147. 10.1016/j.heares.2017.01.003 [PubMed: 28087419]
131. Liu X, Heidelberger R, Janz R (2014) Phosphorylation of syntaxin 3B by CaMKII regulates the formation of t-SNARE complexes. Mol Cell Neurosci 60:53–62. 10.1016/j.mcn.2014.03.002 [PubMed: 24680688]
132. LoGiudice L, Sterling P, Matthews G (2008) Mobility and turnover of vesicles at the synaptic ribbon. J Neurosci 28:3150–3158. 10.1523/JNEUROSCI.5753-07.2008 [PubMed: 18354018]

133. Lohner M, Babai N, Muller T, Gierke K, Atorf J, Joachimsthaler A, Peukert A, Martens H, Feigenspan A, Kremers J, Schoch S, Brandstatter JH, Regus-Leidig H (2017) Analysis of RIM expression and function at mouse photoreceptor ribbon synapses. J Neurosci 37:7848–7863. 10.1523/JNEUROSCI.2795-16.2017 [PubMed: 28701482]

134. Lv C, Gould TJ, Bewersdorf J, Zenisek D (2012) High-resolution optical imaging of zebrafish larval ribbon synapse protein RIBEYE, RIM2, and CaV 1.4 by stimulation emission depletion microscopy. Microsc Microanal 18:745–752. 10.1017/S1431927612000268 [PubMed: 22832038]

135. MacLeish PR, Nurse CA (2007) Ion channel compartments in photoreceptors: evidence from salamander rods with intact and ablated terminals. J Neurophysiol 98:86–95. 10.1152/jn.00775.2006 [PubMed: 17460105]

136. Maddox JW, Randall KL, Yadav RP, Williams B, Hagen J, Derr PJ, Kerov V, Della Santina L, Baker SA, Artemyev N, Hoon M, Lee A (2020) A dual role for Cav1.4 Ca(2+) channels in the molecular and structural organization of the rod photoreceptor synapse. Elife 9. 10.7554/eLife.62184

137. Magupalli VG, Schwarz K, Alpadi K, Natarajan S, Seigel GM, Schmitz F (2008) Multiple RIBEYE-RIBEYE interactions create a dynamic scaffold for the formation of synaptic ribbons. J Neurosci 28:7954–7967. 10.1523/JNEUROSCI.1964-08.2008 [PubMed: 18685021]

138. Mandell JW, Townes-Anderson E, Czernik AJ, Cameron R, Greengard P, De Camilli P (1990) Synapsins in the vertebrate retina: absence from ribbon synapses and heterogeneous distribution among conventional synapses. Neuron 5:19–33. 10.1016/0896-6273(90)90030-j [PubMed: 2114884]

139. Maple BR, Werblin FS, Wu SM (1994) Miniature excitatory postsynaptic currents in bipolar cells of the tiger salamander retina. Vision Res 34:2357–2362. 10.1016/0042-6989(94)90281-x [PubMed: 7975276]

140. Mataruga A, Kremmer E, Muller F (2007) Type 3a and type 3b OFF cone bipolar cells provide for the alternative rod pathway in the mouse retina. J Comp Neurol 502:1123–1137. 10.1002/cne.21367 [PubMed: 17447251]

141. Maxeiner S, Luo F, Tan A, Schmitz F, Sudhof TC (2016) How to make a synaptic ribbon: RIBEYE deletion abolishes ribbons in retinal synapses and disrupts neurotransmitter release. EMBO J 35:1098–1114. 10.15252/embj.201592701 [PubMed: 26929012]

142. McRory JE, Hamid J, Doering CJ, Garcia E, Parker R, Hamming K, Chen L, Hildebrand M, Beedle AM, Feldcamp L, Zamponi GW, Snutch TP (2004) The CACNA1F gene encodes an L-type calcium channel with unique biophysical properties and tissue distribution. J Neurosci 24:1707–1718. 10.1523/JNEUROSCI.4846-03.2004 [PubMed: 14973233]

143. Mehta B, Ke JB, Zhang L, Baden AD, Markowitz AL, Nayak S, Briggman KL, Zenisek D, Singer JH (2014) Global Ca^{2+} signaling drives ribbon-independent synaptic transmission at rod bipolar cell synapses. J Neurosci 34:6233–6244. 10.1523/JNEUROSCI.5324-13.2014 [PubMed: 24790194]

144. Mehta B, Snellman J, Chen S, Li W, Zenisek D (2013) Synaptic ribbons influence the size and frequency of miniature-like evoked postsynaptic currents. Neuron 77:516–527. 10.1016/j.neuron.2012.11.024 [PubMed: 23395377]

145. Mercer AJ, Chen M, Thoreson WB (2011) Lateral mobility of presynaptic L-type calcium channels at photoreceptor ribbon synapses. J Neurosci 31:4397–4406. 10.1523/JNEUROSCI.5921-10.2011 [PubMed: 21430141]

146. Mercer AJ, Rabl K, Riccardi GE, Brecha NC, Stella SL Jr, Thoreson WB (2011) Location of release sites and calcium-activated chloride channels relative to calcium channels at the photoreceptor ribbon synapse. J Neurophysiol 105:321–335. 10.1152/jn.00332.2010 [PubMed: 21084687]

147. Mercer AJ, Szalewski RJ, Jackman SL, Van Hook MJ, Thoreson WB (2012) Regulation of presynaptic strength by controlling Ca^{2+} channel mobility: effects of cholesterol depletion on release at the cone ribbon synapse. J Neurophysiol 107:3468–3478. 10.1152/jn.00779.2011 [PubMed: 22442573]

148. Midorikawa M, Tsukamoto Y, Berglund K, Ishii M, Tachibana M (2007) Different roles of ribbon-associated and ribbon-free active zones in retinal bipolar cells. Nat Neurosci 10:1268–1276. 10.1038/nn1963 [PubMed: 17828257]

149. Migdale K, Herr S, Klug K, Ahmad K, Linberg K, Sterling P, Schein S (2003) Two ribbon synaptic units in rod photoreceptors of macaque, human, and cat. J Comp Neurol 455:100–112. 10.1002/cne.10501 [PubMed: 12454999]

150. Miki T, Midorikawa M, Sakaba T (2020) Direct imaging of rapid tethering of synaptic vesicles accompanying exocytosis at a fast central synapse. Proc Natl Acad Sci U S A 117:14493–14502. 10.1073/pnas.2000265117 [PubMed: 32513685]

151. Morgans CW, Brandstatter JH, Kellerman J, Betz H, Wassle H (1996) A SNARE complex containing syntaxin 3 is present in ribbon synapses of the retina. J Neurosci 16:6713–6721. 10.1523/JNEUROSCI.16-21-06713.1996 [PubMed: 8824312]

152. Mortensen LS, Park SJH, Ke JB, Cooper BH, Zhang L, Imig C, Lowel S, Reim K, Brose N, Demb JB, Rhee JS, Singer JH (2016) Complexin 3 increases the fidelity of signaling in a retinal circuit by regulating exocytosis at ribbon synapses. Cell Rep 15:2239–2250. 10.1016/j.celrep.2016.05.012 [PubMed: 27239031]

153. Moser T, Grabner CP, Schmitz F (2020) Sensory processing at ribbon synapses in the retina and the cochlea. Physiol Rev 100:103–144. 10.1152/physrev.0026.2018 [PubMed: 31373863]

154. Muller TM, Gierke K, Joachimsthaler A, Sticht H, Izsvak Z, Hamra FK, Fejtova A, Ackermann F, Garner CC, Kremers J, Brandstatter JH, Regus-Leidig H (2019) A multiple piccolino-RIBEYE interaction supports plate-shaped synaptic ribbons in retinal neurons. J Neurosci 39:2606–2619. 10.1523/JNEUROSCI.2038-18.2019 [PubMed: 30696732]

155. Muresan V, Lyass A, Schnapp BJ (1999) The kinesin motor KIF3A is a component of the presynaptic ribbon in vertebrate photoreceptors. J Neurosci 19:1027–1037. 10.1523/JNEUROSCI.19-03-01027.1999 [PubMed: 9920666]

156. Murthy VN, Stevens CF (1999) Reversal of synaptic vesicle docking at central synapses. Nat Neurosci 2:503–507. 10.1038/9149 [PubMed: 10448213]

157. Nakakubo Y, Abe S, Yoshida T, Takami C, Isa M, Wojcik SM, Brose N, Takamori S, Hori T (2020) Vesicular glutamate transporter expression ensures high-fidelity synaptic transmission at the calyx of held synapses. Cell Rep 32:108040. 10.1016/j.celrep.2020.108040 [PubMed: 32814044]

158. Oesch NW, Diamond JS (2011) Ribbon synapses compute temporal contrast and encode luminance in retinal rod bipolar cells. Nat Neurosci 14:1555–1561. 10.1038/nn.2945 [PubMed: 22019730]

159. Ohmori H, Yoshii M (1977) Surface potential reflected in both gating and permeation mechanisms of sodium and calcium channels of the tunicate egg cell membrane. J Physiol 267:429–463. 10.1113/jphysiol.1977.sp011821 [PubMed: 17734]

160. Okawa H, Sampath AP, Laughlin SB, Fain GL (2008) ATP consumption by mammalian rod photoreceptors in darkness and in light. Curr Biol 18:1917–1921. 10.1016/j.cub.2008.10.029 [PubMed: 19084410]

161. Okawa H, Yu WQ, Matti U, Schwarz K, Odermatt B, Zhong H, Tsukamoto Y, Lagnado L, Rieke F, Schmitz F, Wong ROL (2019) Dynamic assembly of ribbon synapses and circuit maintenance in a vertebrate sensory system. Nat Commun 10:2167. 10.1038/s41467-019-10123-1 [PubMed: 31092821]

162. Pahlberg J, Sampath AP (2011) Visual threshold is set by linear and nonlinear mechanisms in the retina that mitigate noise: how neural circuits in the retina improve the signal-to-noise ratio of the single-photon response. BioEssays 33:438–447. 10.1002/bies.201100014 [PubMed: 21472740]

163. Pang JJ, Gao F, Barrow A, Jacoby RA, Wu SM (2008) How do tonic glutamatergic synapses evade receptor desensitization? J Physiol 586:2889–2902. 10.1113/jphysiol.2008.151050 [PubMed: 18420706]

164. Pangrsic T, Singer JH, Koschak A (2018) Voltage-gated calcium channels: key players in sensory coding in the retina and the inner ear. Physiol Rev 98:2063–2096. 10.1152/physrev.00030.2017 [PubMed: 30067155]

165. Piano I, Novelli E, Della Santina L, Strettoi E, Cervetto L, Gargini C (2016) Involvement of autophagic pathway in the progression of retinal degeneration in a mouse model of diabetes. Front Cell Neurosci 10:42. 10.3389/fncel.2016.00042 [PubMed: 26924963]
166. Picaud SA, Larsson HP, Grant GB, Lecar H, Werblin FS (1995) Glutamate-gated chloride channel with glutamate-transporter-like properties in cone photoreceptors of the tiger salamander. J Neurophysiol 74:1760–1771. 10.1152/jn.1995.74.4.1760 [PubMed: 8989410]
167. Piccolino M, Vellani V, Rakotobe LA, Pignatelli A, Barnes S, McNaughton P (1999) Manipulation of synaptic sign and strength with divalent cations in the vertebrate retina: pushing the limits of tonic, chemical neurotransmission. Eur J Neurosci 11:4134–4138. 10.1046/j.1460-9568.1999.00842.x [PubMed: 10583501]
168. Pierantoni RL (1984) A quantitative study on synaptic ribbons in the photoreceptors of turtle and frog. In: Borsellino ACL (ed) Photoreceptors. NATO Asi Series (Series A: Life Sciences), vol 75. Boston: Springer, pp 255–283. 10.1007/978-1-4615-9382-9
169. Prevo B, Scholey JM, Peterman EJG (2017) Intraflagellar transport: mechanisms of motor action, cooperation, and cargo delivery. FEBS J 284:2905–2931. 10.1111/febs.14068 [PubMed: 28342295]
170. Rabl K, Cadetti L, Thoreson WB (2005) Kinetics of exocytosis is faster in cones than in rods. J Neurosci 25:4633–4640. 10.1523/JNEUROSCI.4298-04.2005 [PubMed: 15872111]
171. Rabl K, Cadetti L, Thoreson WB (2006) Paired-pulse depression at photoreceptor synapses. J Neurosci 26:2555–2563. 10.1523/JNEUROSCI.3667-05.2006 [PubMed: 16510733]
172. Rabl K, Thoreson WB (2002) Calcium-dependent inactivation and depletion of synaptic cleft calcium ions combine to regulate rod calcium currents under physiological conditions. Eur J Neurosci 16:2070–2077. 10.1046/j.1460-9568.2002.02277.x [PubMed: 12473074]
173. Rao-Mirotznik R, Harkins AB, Buchsbaum G, Sterling P (1995) Mammalian rod terminal: architecture of a binary synapse. Neuron 14:561–569. 10.1016/0896-6273(95)90312-7 [PubMed: 7695902]
174. Rao R, Buchsbaum G, Sterling P (1994) Rate of quantal transmitter release at the mammalian rod synapse. Biophys J 67:57–63. 10.1016/S0006-3495(94)80454-0 [PubMed: 7919023]
175. Raviola E, Gilula NB (1975) Intramembrane organization of specialized contacts in the outer plexiform layer of the retina. A freeze-fracture study in monkeys and rabbits. J Cell Biol 65:192–222 [PubMed: 1127010]
176. Rea R, Li J, Dharia A, Levitan ES, Sterling P, Kramer RH (2004) Streamlined synaptic vesicle cycle in cone photoreceptor terminals. Neuron 41:755–766. 10.1016/s0896-6273(04)00088-1 [PubMed: 15003175]
177. Reim K, Wegmeyer H, Brandstatter JH, Xue M, Rosenmund C, Dresbach T, Hofmann K, Brose N (2005) Structurally and functionally unique complexins at retinal ribbon synapses. J Cell Biol 169:669–680. 10.1083/jcb.200502115 [PubMed: 15911881]
178. Reme CE, Young RW (1977) The effects of hibernation on cone visual cells in the ground squirrel. Invest Ophthalmol Vis Sci 16:815–840 [PubMed: 893032]
179. Rhee JS, Li LY, Shin OH, Rah JC, Rizo J, Sudhof TC, Rosenmund C (2005) Augmenting neurotransmitter release by enhancing the apparent Ca^{2+} affinity of synaptotagmin 1. Proc Natl Acad Sci U S A 102:18664–18669. 10.1073/pnas.0509153102 [PubMed: 16352718]
180. Rieke F, Schwartz EA (1996) Asynchronous transmitter release: control of exocytosis and endocytosis at the salamander rod synapse. J Physiol 493(Pt 1):1–8. 10.1113/jphysiol.1996.sp021360 [PubMed: 8735690]
181. Sampath AP, Rieke F (2004) Selective transmission of single photon responses by saturation at the rod-to-rod bipolar synapse. Neuron 41:431–443. 10.1016/s0896-6273(04)00005-4 [PubMed: 14766181]
182. Sang L, Dick IE, Yue DT (2016) Protein kinase A modulation of CaV1.4 calcium channels. Nat Commun 7:12239–12443. 10.1038/ncomms12239 [PubMed: 27456671]
183. Schein S, Ahmad KM (2005) A clockwork hypothesis: synaptic release by rod photoreceptors must be regular. Biophys J 89:3931–3949. 10.1529/biopsysj.105.070623 [PubMed: 16169984]
184. Schlamp CL, Williams DS (1996) Myosin V in the retina: localization in the rod photoreceptor synapse. Exp Eye Res 63:613–619. 10.1006/exer.1996.0155 [PubMed: 9068368]

185. Schmitz F (2009) The making of synaptic ribbons: how they are built and what they do. Neuroscientist 15:611–624. 10.1177/1073858409340253 [PubMed: 19700740]

186. Schmitz F, Konigstorfer A, Sudhof TC (2000) RIBEYE, a component of synaptic ribbons: a protein's journey through evolution provides insight into synaptic ribbon function. Neuron 28:857–872. 10.1016/s0896-6273(00)00159-8 [PubMed: 11163272]

187. Schmitz Y, Witkovsky P (1997) Dependence of photoreceptor glutamate release on a dihydropyridine-sensitive calcium channel. Neuroscience 78:1209–1216. 10.1016/s0306-4522(96)00678-1 [PubMed: 9174087]

188. Schneeweis DM, Schnapf JL (1995) Photovoltage of rods and cones in the macaque retina. Science 268:1053–1056. 10.1126/science.7754386 [PubMed: 7754386]

189. Schneggenburger R, Rosenmund C (2015) Molecular mechanisms governing Ca(2+) regulation of evoked and spontaneous release. Nat Neurosci 18:935–941. 10.1038/nn.4044 [PubMed: 26108721]

190. Schwarz K, Natarajan S, Kassas N, Vitale N, Schmitz F (2011) The synaptic ribbon is a site of phosphatidic acid generation in ribbon synapses. J Neurosci 31:15996–16011. 10.1523/JNEUROSCI.2965-11.2011 [PubMed: 22049442]

191. Sheng Z, Choi SY, Dharia A, Li J, Sterling P, Kramer RH (2007) Synaptic Ca^{2+} in darkness is lower in rods than cones, causing slower tonic release of vesicles. J Neurosci 27:5033–5042. 10.1523/JNEUROSCI.5386-06.2007 [PubMed: 17494689]

192. Sherry DM, Heidelberger R (2005) Distribution of proteins associated with synaptic vesicle endocytosis in the mouse and goldfish retina. J Comp Neurol 484:440–457. 10.1002/cne.20504 [PubMed: 15770653]

193. Sjostrand FS (1958) Ultrastructure of retinal rod synapses of the guinea pig eye as revealed by three-dimensional reconstructions from serial sections. J Ultrastruct Res 2:122–170. 10.1016/s0022-5320(58)90050-9 [PubMed: 13631744]

194. Snellman J, Mehta B, Babai N, Bartoletti TM, Akmentin W, Francis A, Matthews G, Thoreson W, Zenisek D (2011) Acute destruction of the synaptic ribbon reveals a role for the ribbon in vesicle priming. Nat Neurosci 14:1135–1141. 10.1038/nn.2870 [PubMed: 21785435]

195. Spiwoks-Becker I, Glas M, Lasarzik I, Vollrath L (2004) Mouse photoreceptor synaptic ribbons lose and regain material in response to illumination changes. Eur J Neurosci 19:1559–1571. 10.1111/j.1460-9568.2004.03198.x [PubMed: 15066152]

196. Stankiewicz TR, Gray JJ, Winter AN, Linseman DA (2014) C-terminal binding proteins: central players in development and disease. Biomol Concepts 5:489–511. 10.1515/bmc-2014-0027 [PubMed: 25429601]

197. Stanley EF (2000) Presynaptic calcium channels and the depletion of synaptic cleft calcium ions. J Neurophysiol 83:477–482. 10.1152/jn.2000.83.1.477 [PubMed: 10634889]

198. Steele EC Jr, Chen X, Iuvone PM, MacLeish PR (2005) Imaging of Ca^{2+} dynamics within the presynaptic terminals of salamander rod photoreceptors. J Neurophysiol 94:4544–4553. 10.1152/jn.01193.2004 [PubMed: 16107525]

199. Sterling P, Laughlin S (2015) Principles of neural design. Cambridge: MIT Press. 10.7551/mitpress/9780262028707.001.0001

200. Sterling P, Matthews G (2005) Structure and function of ribbon synapses. Trends Neurosci 28:20–29. 10.1016/j.tins.2004.11.009 [PubMed: 15626493]

201. Stohr H, Heisig JB, Benz PM, Schoberl S, Milenkovic VM, Strauss O, Aartsen WM, Wijnholds J, Weber BH, Schulz HL (2009) TMEM16B, a novel protein with calcium-dependent chloride channel activity, associates with a presynaptic protein complex in photoreceptor terminals. J Neurosci 29:6809–6818. 10.1523/JNEUROSCI.5546-08.2009 [PubMed: 19474308]

202. Suryanarayanan A, Slaughter MM (2006) Synaptic transmission mediated by internal calcium stores in rod photoreceptors. J Neurosci 26:1759–1766. 10.1523/JNEUROSCI.3895-05.2006 [PubMed: 16467524]

203. Szikra T, Barabas P, Bartoletti TM, Huang W, Akopian A, Thoreson WB, Krizaj D (2009) Calcium homeostasis and cone signaling are regulated by interactions between calcium stores and plasma membrane ion channels. PLoS ONE 4:e6723. 10.1371/journal.pone.0006723 [PubMed: 19696927]

204. Szikra T, Cusato K, Thoreson WB, Barabas P, Bartoletti TM, Krizaj D (2008) Depletion of calcium stores regulates calcium influx and signal transmission in rod photoreceptors. J Physiol 586:4859–4875. 10.1113/jphysiol.2008.160051 [PubMed: 18755743]

205. Szmajda BA, Devries SH (2011) Glutamate spillover between mammalian cone photoreceptors. J Neurosci 31:13431–13441. 10.1523/JNEUROSCI.2105-11.2011 [PubMed: 21940436]

206. Tan GM, Yu D, Wang J, Soong TW (2012) Alternative splicing at C terminus of Ca(V)1.4 calcium channel modulates calcium-dependent inactivation, activation potential, and current density. J Biol Chem 287:832–847. 10.1074/jbc.M111.268722 [PubMed: 22069316]

207. Thoreson WB, Babai N, Bartoletti TM (2008) Feedback from horizontal cells to rod photoreceptors in vertebrate retina. J Neurosci 28:5691–5695. 10.1523/JNEUROSCI.0403-08.2008 [PubMed: 18509030]

208. Thoreson WB, Bryson EJ (2004) Chloride equilibrium potential in salamander cones. BMC Neurosci 5:53. 10.1186/1471-2202-5-53 [PubMed: 15579212]

209. Thoreson WB, Bryson EJ, Rabl K (2003) Reciprocal interactions between calcium and chloride in rod photoreceptors. J Neurophysiol 90:1747–1753. 10.1152/jn.00932.2002 [PubMed: 12724369]

210. Thoreson WB, Burkhardt DA (2003) Contrast encoding in retinal bipolar cells: current vs. voltage. Vis Neurosci 20:19–28. 10.1017/s0952523803201036 [PubMed: 12699080]

211. Thoreson WB, Dacey DM (2019) Diverse cell types, circuits, and mechanisms for color vision in the vertebrate retina. Physiol Rev 99:1527–1573. 10.1152/physrev.00027.2018 [PubMed: 31140374]

212. Thoreson WB, Mangel SC (2012) Lateral interactions in the outer retina. Prog Retin Eye Res 31:407–441. 10.1016/j.preteyeres.2012.04.003 [PubMed: 22580106]

213. Thoreson WB, Nitzan R, Miller RF (1997) Reducing extracellular Cl- suppresses dihydropyridine-sensitive Ca^{2+} currents and synaptic transmission in amphibian photoreceptors. J Neurophysiol 77:2175–2190. 10.1152/jn.1997.77.4.2175 [PubMed: 9114264]

214. Thoreson WB, Nitzan R, Miller RF (2000) Chloride efflux inhibits single calcium channel open probability in vertebrate photoreceptors: chloride imaging and cell-attached patch-clamp recordings. Vis Neurosci 17:197–206. 10.1017/s0952523800172025 [PubMed: 10824674]

215. Thoreson WB, Rabl K, Townes-Anderson E, Heidelberger R (2004) A highly Ca^{2+}-sensitive pool of vesicles contributes to linearity at the rod photoreceptor ribbon synapse. Neuron 42:595–605. 10.1016/s0896-6273(04)00254-5 [PubMed: 15157421]

216. Thoreson WB, Stella SL (2000) Anion modulation of calcium current voltage dependence and amplitude in salamander rods. Biochim Biophys Acta 1464:142–150. 10.1016/s0005-2736(99)00257-6 [PubMed: 10704928]

217. Thoreson WB, Tranchina D, Witkovsky P (2003) Kinetics of synaptic transfer from rods and cones to horizontal cells in the salamander retina. Neuroscience 122:785–798. 10.1016/j.neuroscience.2003.08.012 [PubMed: 14622921]

218. Thoreson WB, Van Hook MJ, Parmelee C, Curto C (2016) Modeling and measurement of vesicle pools at the cone ribbon for voltage-dependent changes in release. Synapse 70:1–14. 10.1002/syn.21871 [PubMed: 26541100]

219. Tian M, Xu CS, Montpetit R, Kramer RH (2012) Rab3A mediates vesicle delivery at photoreceptor ribbon synapses. J Neurosci 32:6931–6936. 10.1523/JNEUROSCI.0265-12.2012 [PubMed: 22593061]

220. tom Dieck S, Altrock WD, Kessels MM, Qualmann B, Regus H, Brauner D, Fejtova A, Bracko O, Gundelfinger ED, Brandstatter JH (2005) Molecular dissection of the photoreceptor ribbon synapse: physical interaction of Bassoon and RIBEYE is essential for the assembly of the ribbon complex. J Cell Biol 168:825–836. 10.1083/jcb.200408157 [PubMed: 15728193]

221. tom Dieck S, Specht D, Strenzke NN, Hida Y, Krishnamoorthy V, Schmidt KF, Inoue E, Ishizaki H, Tanaka-Okamoto M, Miyoshi J, Hagiwara A, Brandstatter JH, Lowel S, Gollisch T, Ohtsuka T, Moser T (2012) Deletion of the presynaptic scaffold CAST reduces active zone size in rod photoreceptors and impairs visual processing. J Neurosci 32:12192–12203. 10.1523/JNEUROSCI.0752-12.2012 [PubMed: 22933801]

222. Townes-Anderson E, MacLeish PR, Raviola E (1985) Rod cells dissociated from mature salamander retina: ultrastructure and uptake of horseradish peroxidase. J Cell Biol 100:175–188. 10.1083/jcb.100.1.175 [PubMed: 3965470]

223. Usukura J, Yamada E (1987) Ultrastructure of the synaptic ribbons in photoreceptor cells of Rana catesbeiana revealed by freeze-etching and freeze-substitution. Cell Tissue Res 247:483–488. 10.1007/BF00215740 [PubMed: 3494517]

224. Uthaiah RC, Hudspeth AJ (2010) Molecular anatomy of the hair cell's ribbon synapse. J Neurosci 30:12387–12399. 10.1523/JNEUROSCI.1014-10.2010 [PubMed: 20844134]

225. Vaithianathan T, Akmentin W, Henry D, Matthews G (2013) The ribbon-associated protein C-terminal-binding protein 1 is not essential for the structure and function of retinal ribbon synapses. Mol Vis 19:917–926 [PubMed: 23687428]

226. Vaithianathan T, Henry D, Akmentin W, Matthews G (2015) Functional roles of complexin in neurotransmitter release at ribbon synapses of mouse retinal bipolar neurons. J Neurosci 35:4065–4070. 10.1523/JNEUROSCI.2703-14.2015 [PubMed: 25740533]

227. Vaithianathan T, Henry D, Akmentin W, Matthews G (2016) Nanoscale dynamics of synaptic vesicle trafficking and fusion at the presynaptic active zone. Elife 5. 10.7554/eLife.13245

228. Vaithianathan T, Zanazzi G, Henry D, Akmentin W, Matthews G (2013) Stabilization of spontaneous neurotransmitter release at ribbon synapses by ribbon-specific subtypes of complexin. J Neurosci 33:8216–8226. 10.1523/JNEUROSCI.1280-12.2013 [PubMed: 23658160]

229. Van Hook MJ, Nawy S, Thoreson WB (2019) Voltage-and calcium-gated ion channels of neurons in the vertebrate retina. Prog Retin Eye Res 72:100760. 10.1016/j.preteyeres.2019.05.001 [PubMed: 31078724]

230. Van Hook MJ, Parmelee CM, Chen M, Cork KM, Curto C, Thoreson WB (2014) Calmodulin enhances ribbon replenishment and shapes filtering of synaptic transmission by cone photoreceptors. J Gen Physiol 144:357–378. 10.1085/jgp.201411229 [PubMed: 25311636]

231. Van Hook MJ, Thoreson WB (2012) Rapid synaptic vesicle endocytosis in cone photoreceptors of salamander retina. J Neurosci 32:18112–18123. 10.1523/JNEUROSCI.1764-12.2012 [PubMed: 23238726]

232. Van Hook MJ, Thoreson WB (2014) Endogenous calcium buffering at photoreceptor synaptic terminals in salamander retina. Synapse 68:518–528. 10.1002/syn.21768 [PubMed: 25049035]

233. Van Hook MJ, Thoreson WB (2015) Weak endogenous Ca^{2+} buffering supports sustained synaptic transmission by distinct mechanisms in rod and cone photoreceptors in salamander retina. Physiol Rep 3:e12567. 10.14814/phy2.12567 [PubMed: 26416977]

234. van Rossum MC, Smith RG (1998) Noise removal at the rod synapse of mammalian retina. Vis Neurosci 15:809–821. 10.1017/s0952523898155037 [PubMed: 9764523]

235. Verhage M, Sorensen JB (2008) Vesicle docking in regulated exocytosis. Traffic 9:1414–1424. 10.1111/j.1600-0854.2008.00759.x [PubMed: 18445120]

236. Verweij J, Hornstein EP, Schnapf JL (2003) Surround antagonism in macaque cone photoreceptors. J Neurosci 23:10249–10257. 10.1523/JNEUROSCI.23-32-10249.2003 [PubMed: 14614083]

237. Verweij J, Kamermans M, Spekreijse H (1996) Horizontal cells feed back to cones by shifting the cone calcium-current activation range. Vision Res 36:3943–3953. 10.1016/s0042-6989(96)00142-3 [PubMed: 9068848]

238. Von Kriegstein K, Schmitz F, Link E, Sudhof TC (1999) Distribution of synaptic vesicle proteins in the mammalian retina identifies obligatory and facultative components of ribbon synapses. Eur J Neurosci 11:1335–1348. 10.1046/j.1460-9568.1999.00542.x [PubMed: 10103129]

239. Wahl S, Katiyar R, Schmitz F (2013) A local, periactive zone endocytic machinery at photoreceptor synapses in close vicinity to synaptic ribbons. J Neurosci 33:10278–10300. 10.1523/JNEUROSCI.5048-12.2013 [PubMed: 23785143]

240. Waldner DM, Bech-Hansen NT, Stell WK (2018) Channeling vision: CaV1.4-A critical link in retinal signal transmission. Biomed Res Int 2018:7272630. 10.1155/2018/7272630 [PubMed: 29854783]

241. Wang TM, Holzhausen LC, Kramer RH (2014) Imaging an optogenetic pH sensor reveals that protons mediate lateral inhibition in the retina. Nat Neurosci 17:262–268. 10.1038/nn.3627 [PubMed: 24441679]

242. Wang Y, Fehlhaber KE, Sarria I, Cao Y, Ingram NT, Guerrero-Given D, Throesch B, Baldwin K, Kamasawa N, Ohtsuka T, Sampath AP, Martemyanov KA (2017) The auxiliary calcium channel subunit alpha2delta4 is required for axonal elaboration, synaptic transmission, and wiring of rod photoreceptors. Neuron 93(1359–1374):e1356. 10.1016/j.neuron.2017.02.021

243. Wen X, Saltzgaber GW, Thoreson WB (2017) Kiss-and-run is a significant contributor to synaptic exocytosis and endocytosis in photoreceptors. Front Cell Neurosci 11:286. 10.3389/fncel.2017.00286 [PubMed: 28979188]

244. Wen X, Van Hook MJ, Grassmeyer JJ, Wiesman AI, Rich GM, Cork KM, Thoreson WB (2018) Endocytosis sustains release at photoreceptor ribbon synapses by restoring fusion competence. J Gen Physiol 150:591–611. 10.1085/jgp.201711919 [PubMed: 29555658]

245. Wilhelm BG, Mandad S, Truckenbrodt S, Krohnert K, Schafer C, Rammner B, Koo SJ, Classen GA, Krauss M, Haucke V, Urlaub H, Rizzoli SO (2014) Composition of isolated synaptic boutons reveals the amounts of vesicle trafficking proteins. Science 344:1023–1028. 10.1126/science.1252884 [PubMed: 24876496]

246. Wilkinson MF, Barnes S (1996) The dihydropyridine-sensitive calcium channel subtype in cone photoreceptors. J Gen Physiol 107:621–630. 10.1085/jgp.107.5.621 [PubMed: 8740375]

247. Witkovsky P, Gabriel R, Krizaj D (2008) Anatomical and neuro-chemical characterization of dopaminergic interplexiform processes in mouse and rat retinas. J Comp Neurol 510:158–174. 10.1002/cne.21784 [PubMed: 18615559]

248. Wu SM (2010) Synaptic organization of the vertebrate retina: general principles and species-specific variations: the Friedenwald lecture. Invest Ophthalmol Vis Sci 51:1263–1274. 10.1167/iovs.09-4396

249. Wycisk KA, Zeitz C, Feil S, Wittmer M, Forster U, Neidhardt J, Wissinger B, Zrenner E, Wilke R, Kohl S, Berger W (2006) Mutation in the auxiliary calcium-channel subunit CACNA2D4 causes autosomal recessive cone dystrophy. Am J Hum Genet 79:973–977. 10.1086/508944 [PubMed: 17033974]

250. Zampighi GA, Schietroma C, Zampighi LM, Woodruff M, Wright EM, Brecha NC (2011) Conical tomography of a ribbon synapse: structural evidence for vesicle fusion. PLoS ONE 6:e16944. 10.1371/journal.pone.0016944 [PubMed: 21390245]

251. Zeitz C, Robson AG, Audo I (2015) Congenital stationary night blindness: an analysis and update of genotype-phenotype correlations and pathogenic mechanisms. Prog Retin Eye Res 45:58–110. 10.1016/j.preteyeres.2014.09.001 [PubMed: 25307992]

252. Zenisek D, Davila V, Wan L, Almers W (2003) Imaging calcium entry sites and ribbon structures in two presynaptic cells. J Neurosci 23:2538–2548. 10.1523/JNEUROSCI.23-07-02538.2003 [PubMed: 12684438]

253. Zenisek D, Steyer JA, Almers W (2000) Transport, capture and exocytosis of single synaptic vesicles at active zones. Nature 406:849–854. 10.1038/35022500 [PubMed: 10972279]

254. Zhang J, Tuo J, Cao X, Shen D, Li W, Chan CC (2013) Early degeneration of photoreceptor synapse in Ccl2/Cx3cr1-deficient mice on Crb1(rd8) background. Synapse 67:515–531. 10.1002/syn.21674. [PubMed: 23592324]

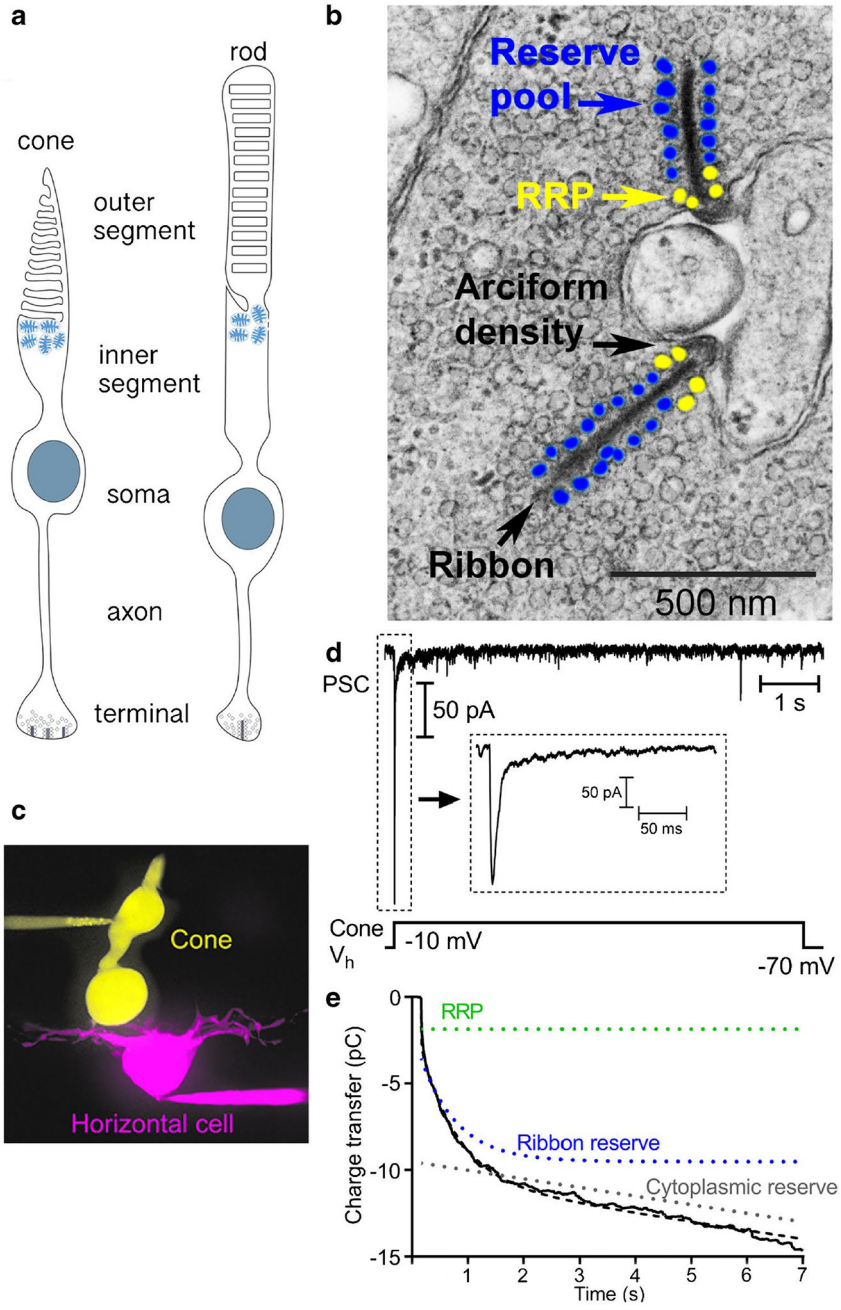

Fig. 1.

Rods, cones, and synaptic vesicle pools at photoreceptor ribbon synapses. **a** Rod and cone anatomy. **b** Electron micrograph of a salamander cone synapse showing two electron-dense ribbons situated above their arciform densities. The readily releasable pool (RRP) of vesicles at the base of each ribbon is colored in yellow. The ribbon-attached reserve pool is shown in blue. Many vesicles surround both sides of the ribbon, forming a cytoplasmic pool. **c** Confocal image of a salamander cone (yellow) and horizontal cell (magenta) filled with Lucifer yellow and sulfarhodamine B, respectively, during paired whole cell recording. **d** Post-synaptic current (PSC) recorded in a horizontal cell evoked by a long depolarizing

step applied to a presynaptic cone. Inset shows a magnified view of the initial transient component of the PSC (adapted from [19]). **e** Charge transfer from the PSC in D was fit with a function consisting of two exponentials and a straight line. The initial fast component corresponds to the RRP, the second slower component likely reflects a ribbon reserve pool, and the linear function likely represents replenishment from the cytoplasmic reserve

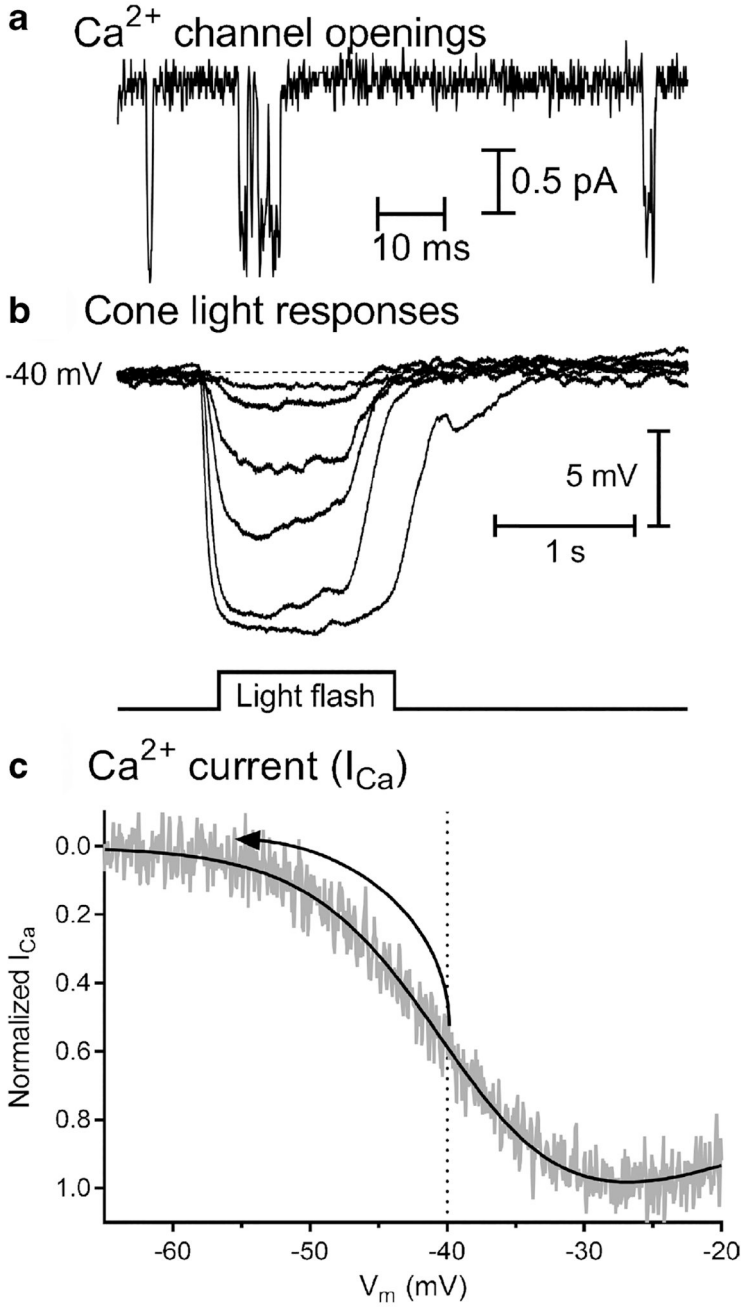

Fig. 2.

Changes in Ca^{2+} channel activity during light-evoked voltage responses of photoreceptors. **a** Ca^{2+} channel openings recorded in the cell-attached patch mode from a photoreceptor terminal in salamander retina with 82 mM Ba^{2+} in the pipette. **b** Overlaid series of voltage responses evoked in a salamander cone by light flashes of increasing intensity. **c** Whole-cell Ca^{2+} current (I_{Ca}) plotted against voltage evoked by a ramp voltage protocol in a cone. Voltage was corrected for access resistance and liquid junction potential [79]. The vertical dashed line indicates the typical photoreceptor resting potential in darkness of − 40 mV. The arrow shows the reduction in I_{Ca} that would accompany a bright light flash

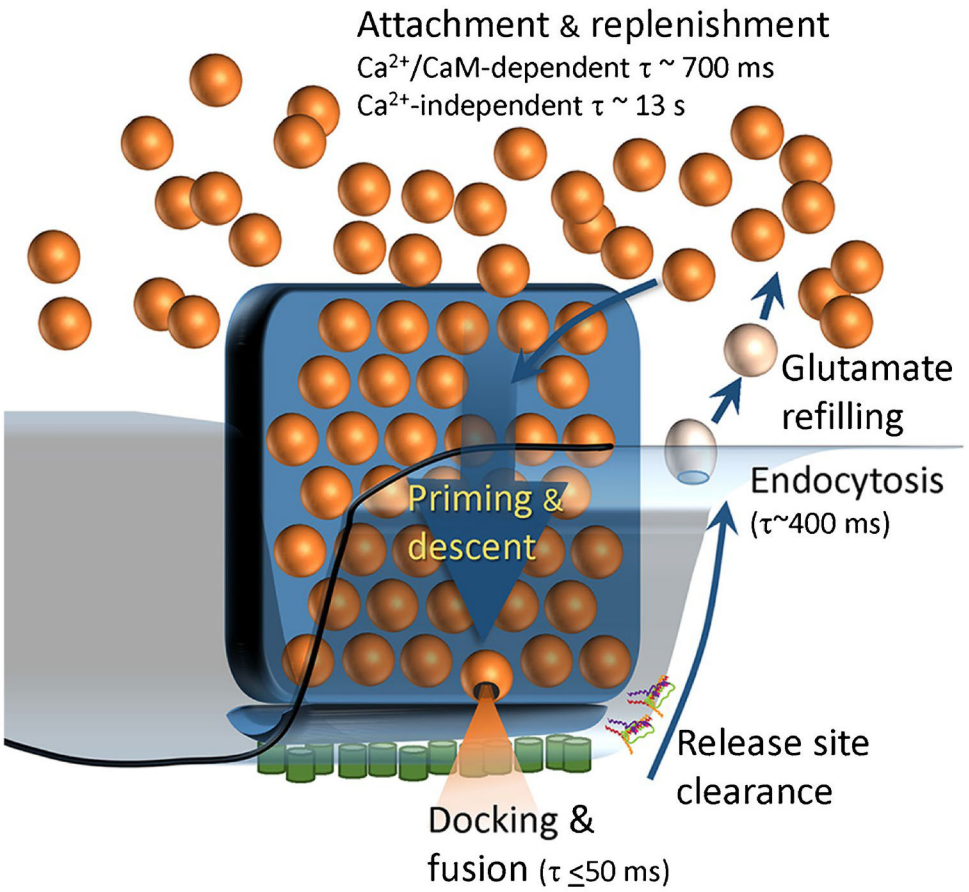

Fig. 3.

Diagram of the vesicle cycle at a photoreceptor ribbon synapse. Vesicles in the readily releasable pool (RRP)at the base of the ribbon dock at the membrane and can fuse within ~ 50 ms. Vesicular proteins and lipids released into the membrane must then be removed to prepare the release site for further release. This involves rapid endocytosis with a time constant (τ) of ~ 400 ms. After reforming and refilling vesicles with glutamate, they are returned to the large cytoplasmic pool of vesicles. Vacant sites on the ribbon are replenished from the cytoplasmic pool via both a rapid Ca^{2+}-/CaM-dependent mechanism (τ ~ 700 ms) and slower Ca^{2+}-independent mechanism (τ ~ 13 s). As vesicles move down the ribbon, they are primed for release. Illustration redrawn and adapted from [230]

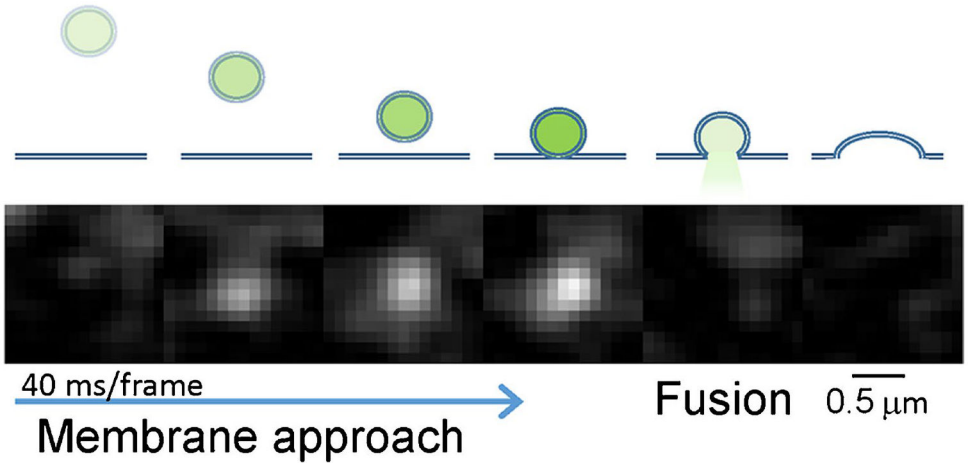

Fig. 4.

Imaging synaptic vesicle approach to the membrane in a salamander rod terminal. Total internal reflectance fluorescence microscopy (TIRFM) was used to image a vesicle approaching the membrane and then fusing at a rod synapse. The vesicle was loaded with 3kD dextran-conjugated AlexaFluor488. The diagram at the top illustrates a vesicle becoming progressively brighter as it advances towards the membrane through the evanescent field generated by TIRF illumination (length constant = 60 nm). As shown by the TIRFM images at the bottom, after approaching the membrane, the vesicle fused and rapidly released its contents, disappearing within a single 40 ms frame [244]

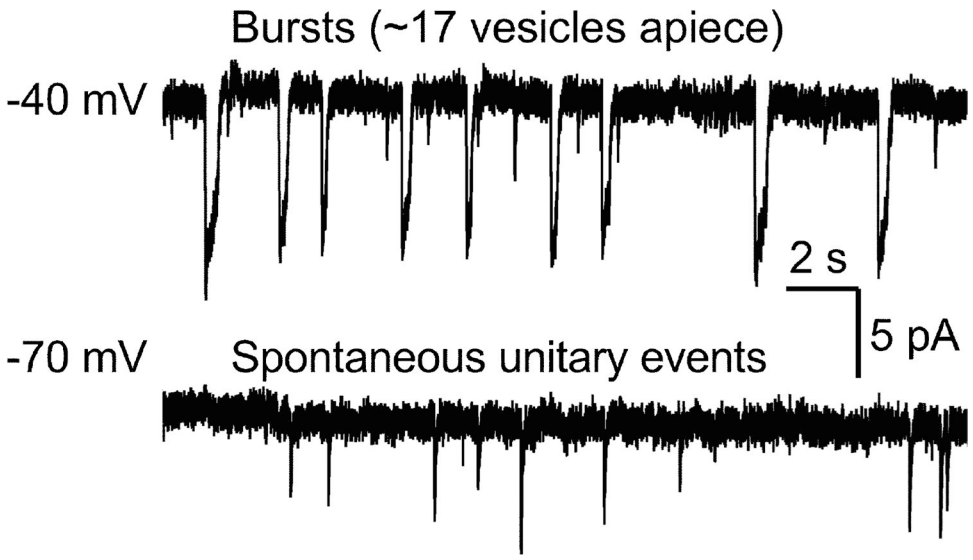

Fig. 5.

Spontaneous and evoked glutamate release from a mouse rod. Glutamate release was assessed in rods by recording anion currents activated during glutamate re-uptake through presynaptic glutamate transporters. When the rod was held at − 70 mV, release consisted of occasional spontaneous, uniquantal events (bottom trace). When this rod was held at − 40 mV, release transitioned to a semi-regular series of multiquantal bursts consisting of ~ 17 vesicles apiece (top trace)